

NPS ARCHIVE
1962
VAN HOOFF, E.

A STUDY OF THE DAMPING CHARACTERISTICS OF
HONEYCOMB SANDWICH CONSTRUCTION

EUGENE R. VAN HOOFF

LIBRARY
U.S. NAVAL POSTGRADUATE SCHOOL
MONTEREY CALIFORNIA

A STUDY OF THE DAMPING
CHARACTERISTICS OF
HONEYCOMB SANDWICH
CONSTRUCTION

* * * * *

Eugene R. Van Hoof

A STUDY OF THE DAMPING
CHARACTERISTICS OF
HONEYCOMB SANDWICH
CONSTRUCTION

by

Eugene R. Van Hoof
"

Lieutenant, United States Navy

Submitted in partial fulfillment of
the requirements for the degree of

MASTER OF SCIENCE
IN
MECHANICAL ENGINEERING

United States Naval Postgraduate School
Monterey, California

1 9 6 2

2. ALIVE

~~145~~

62

AN HOOFF, E.

LIBRARY
U.S. NAVAL POSTGRADUATE SCHOOL
MONTEREY, CALIFORNIA

A STUDY OF THE DAMPING
CHARACTERISTICS OF
HONEYCOMB SANDWICH
CONSTRUCTION

by .

Eugene R. Van Hoof

This work is accepted as fulfilling
the thesis requirements for the degree of
MASTER OF SCIENCE
IN
MECHANICAL ENGINEERING
from the

United States Naval Postgraduate School

ABSTRACT

Damping characteristics of honeycomb sandwich construction are studied experimentally. Tests are made on a series of constant section cantilever beams with aluminum alloy facings and cores. The beams have equal depths, but have a range of core heights varying from 0 (solid beam) to 0.8 of the beam depth. The resonant amplification factor in forced vibration and the logarithmic decrement in free vibration are found for the fundamental mode.

A theoretical analysis is performed, based on the hypothesis that the specific energy dissipation varies as some power (the damping exponent) of the maximum cyclic stress. Experimental results show qualitative agreement with predicted effects of core height variation. Amplitude dependence of observed damping indicates that the damping exponent is between two and three. Measured natural frequencies agree well with calculated values.

ACKNOWLEDGEMENTS

Grateful acknowledgement is extended to Hexcel Products, Inc. of Berkeley, California for furnishing materials used in this project and to Mr. Mahmoud I. Kazimi of Hexcel for technical advice.

Sincerest appreciation is also extended to Prof. R. E. Newton, Chairman, Department of Mechanical Engineering, U.S. Naval Postgraduate School, under whose guidance and assistance this work was carried out; and to my wife, Joy, for her assistance in typing.

TABLE OF CONTENTS

Section	Title	Page
	Abstract	ii
	Acknowledgements	iii
	List of Illustrations	v
	List of Symbols and Abbreviations	vii
1	Introduction	1
2	Experimental Method	7
3	Experimental Results	11
4	Conclusions	18
	Bibliography	19
Appendix I	Theoretical Analysis	20
Appendix II	Experimental Apparatus and Procedures	29
Appendix III	Sample Calculations	35
Appendix IV	Reduction of Experimental Data	42

LIST OF ILLUSTRATIONS

Figure		Page
1	Honeycomb Sandwich Construction	5
2	Schematic of Honeycomb Sandwich Beam	6
3	Honeycomb Core	6
4	Graph of Resonant Amplification Factor vs Tip Amplitude of Beam	14
5	Graph of Resonant Amplification Factor vs Tip Amplitude of Solid Beam	15
6	Honeycomb Sandwich Beams	32
7	Steady State Forced Vibration Test Apparatus	33
8	Free Vibration Decay Test Apparatus	34
9-11	Graphs of Amplification Factor vs Frequency	45-47
12	Portion of Oscillograph Record (Traced from original)	52

LIST OF TABLES

Tables	Title	Page
I	Damping Results from Steady State Forced Vibration Test	16
II	Damping Results from Free Vibration Decay Test	16
III	Combined Results of Frequency Measurements	17
IV	Beam Dimensions	36
V	Computed Values for Honeycomb Beam ($r = 0.260$)	36
VI	Steady State Forced Vibration Experimental Data	48-49
VII	Free Vibration Decay Experimental Data	50-51

LIST OF SYMBOLS AND ABBREVIATIONS

A	Amplification factor (ψ_0/a_0)
A_r	Amplification factor at resonance
a_0	Forced vibration amplitude at center of beam (in.)
b	(subscript) bending
D	Specific damping energy (in.-lb/in. ³ cycle)
D_0	Damping energy (in.-lb/cycle)
E	Modulus of elasticity (psi)
e	(subscript) equivalent width
f	Frequency (cps)
f_n	Resonant frequency (cps)
G	Shear modulus (psi)
I	Moment of inertia (in. ⁴)
J	Damping constant (psi ⁿ⁻¹)
k	Ratio of pure shear to uniaxial tension to produce the same distortion energy
ℓ	Length of beam (in.)
M	Bending moment (in.-lb)
n	Damping exponent
P	Force (lb)
r	Ratio of core thickness to total beam thickness
s	(subscript) shear
t	Total beam thickness (in.)
t_c	Core thickness (in.)
U	Elastic strain energy (in.-lb)

U_0	Total elastic strain energy at maximum stress (in.-lb)
V	Volume (in. ³)
V_s	Shearing force (lb)
W	Weight of beam (lb)
x, y	Cartesian coordinates
X_0, X_1, \dots, X_n	Amplitudes of vibrations (in.)
y_0	Amplitude of vibration at tip of beam (in.)
w	Width of beam (in.)
w_e	Equivalent width of core (in.)
β	Ratio of shear strain energy to bending strain energy
ϵ	Strain
Λ	Shear distribution factor
ρ_{al}	Specific weight of alloy (lb/in. ³)
ρ_c	Specific weight of core (lb/in. ³)
σ	Bending stress (psi)
μ	Mass per unit length of beam (lb-sec ² /in. ²)
ω	Circular frequency (rad/sec)

1. Introduction

Honeycomb sandwich construction, as originally conceived, was intended to increase the strength-to-weight ratio of structures. The theory of the individual components may best be described by making an analogy to an I-beam. The high density facings (see Figs. 1-3 for nomenclature) of a sandwich beam correspond to the flanges of an I-beam; the object being to place a high density, high strength material as far from the neutral axis as possible, thus increasing the section modulus. The honeycomb core is comparable to the web of an I-beam which supports the flanges and acts to carry shear stresses. The honeycomb core maintains continuous support of the facings and may be bonded to the facings by cementing or brazing.

The results of uncontrolled resonant vibrations are well known. Design approaches that may be used to avoid detrimental resonance conditions include [1]:¹

1. Rigidization of structural members.
2. Decoupling of resonating systems.
3. Detuning of coupled resonators.
4. Using high fatigue-strength structural materials.
5. Reducing the vibration excitation of the structure.
6. Incorporating high-energy dissipating mechanisms into the structural fabrication.

All except the last approach have disadvantages for reasons which usually fall into two main categories: the addition of too much weight and ineffective damping over a large frequency spectrum. In contrast, incorporating an energy dissipating mechanism into the structural fabrication will improve structural damping over a broad band of

1

Numbers in brackets refer to entries in the bibliography which appear on page 19.

frequencies [2]. Honeycomb sandwich construction provides such an energy dissipating mechanism. In addition to its main advantage of a high strength-to-weight ratio, the honeycomb core serves as an energy dissipating mechanism which is an integral part of the structure.

There are various methods of specifying damping. The resonant amplification factor A_r is the primary method selected in this study to specify the amount of damping that exists in the honeycomb sandwich material. The resonant amplification may be expressed as [3]:

$$A_r = \frac{2\pi U_o}{D_o} \quad (1)$$

where

U_o = total elastic strain energy at maximum stress (in.-lb)

D_o = damping energy per cycle (in.-lb/cycle)

The damping energy is defined as [3]:

$$D_o = \int D dV \quad (2)$$

where

D = specific damping energy (in.-lb/in.³ cycle)

V = volume (in.³)

The specific damping energy D in a material undergoing cyclic stress is assumed to be expressible as [3]:

$$D = J\sigma^n \quad (3)$$

where

J = material damping constant

n = material damping exponent

σ = maximum cyclic stress

The damping exponent n and damping constant J are considered constants, but they vary with temperature, stress history and stress

level. Study of the effects of temperature and stress history are beyond the scope of this paper; however, at room temperatures and for a moderate stress history no effect is anticipated. Stress level affects this study directly. For many conventional materials $n \approx 3$ for low to intermediate stress levels. For high stress levels (approaching the yield strength) the value of n has been noted as high as 8 [1] [3]. Very low stress levels are used in this study; therefore, the amplification factor is analyzed in Appendix I for damping exponents of two and three. At these low stress levels the damping constant J is assumed constant.

The logarithmic decrement δ specifies the damping in a structural member that is undergoing free vibrations. It is defined in terms of the decay rate of the vibrations by [4]:

$$\delta = \ln \frac{X_n}{X_{n+1}} = \frac{1}{n} \ln \frac{X_0}{X_n} \quad (4)$$

where X represents the general vibration amplitude and n the number of cycles of free vibration for which the amplitude decreases from X_0 to X_n . The logarithmic decrement is thus defined by the relative decrease of the vibration motion over a given number of cycles of vibration.

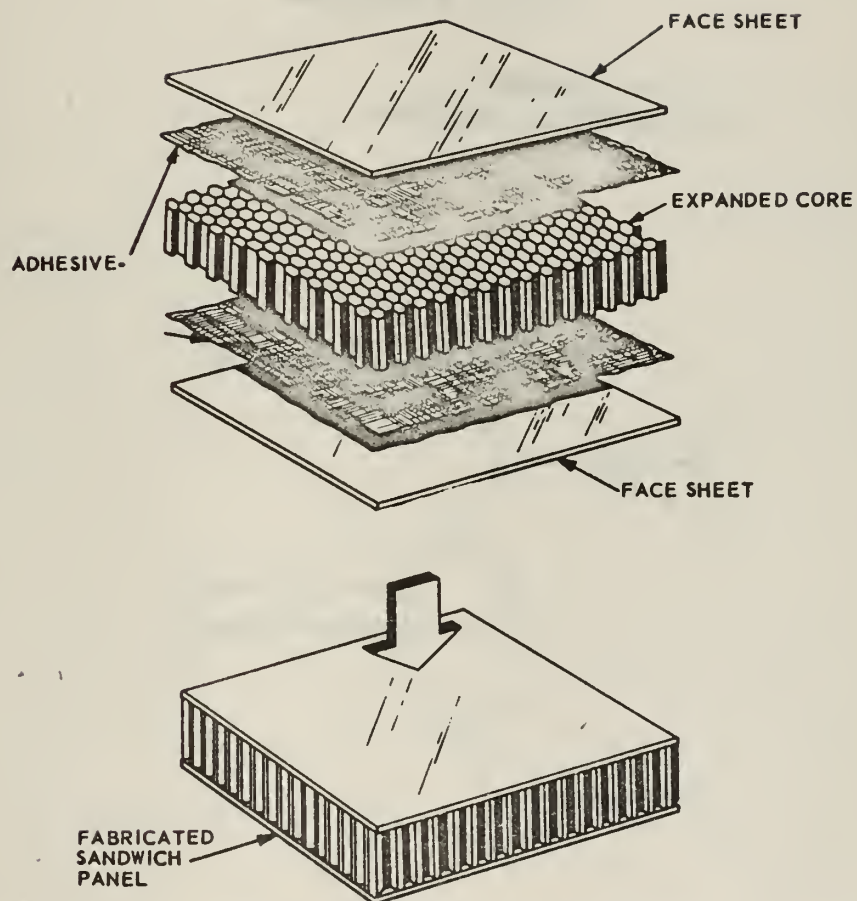
The logarithmic decrement may be related to the selected method of specifying damping in this study, the resonant amplification factor A_r , by the approximation [5]:

$$A_r = \frac{\pi}{\delta - \delta^2} \quad (5)$$

The error in this equation is less than one per cent if the logarithmic decrement is less than 0.12.

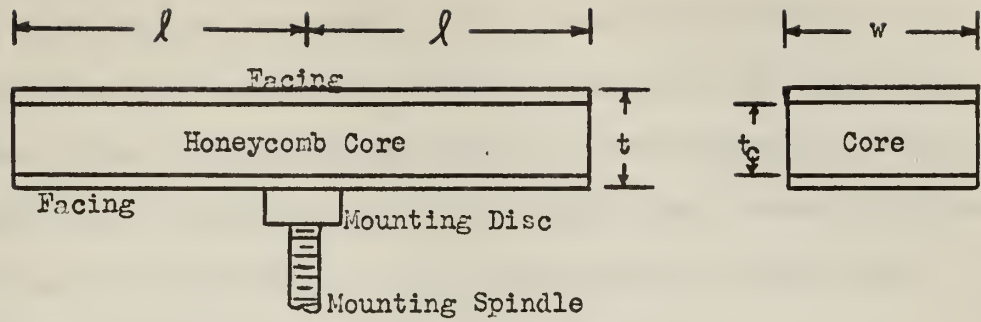
This study is intended to compare theory with experiment, for a

cantilever beam configuration, in order to judge the damping capacity of the honeycomb sandwich material and its variation with core thickness and stress level. From the variation of damping, as specified by the resonant amplification factor with stress level, the material damping exponent n is evaluated to judge the validity of assumed values of two and three for analytical purposes. In addition, the observed natural frequency is compared with the theoretical prediction.



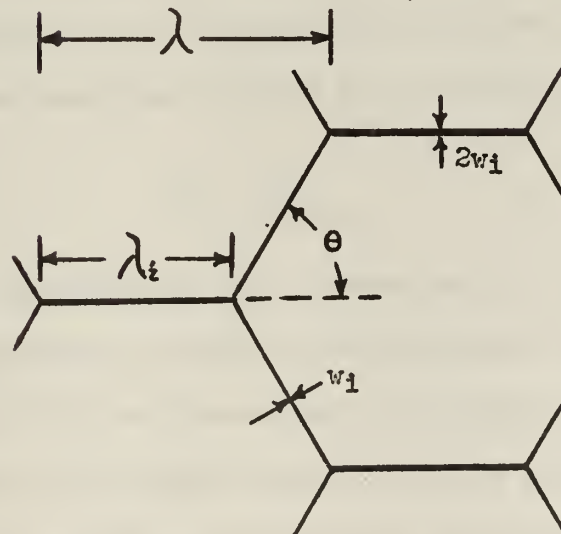
HONEYCOMB SANDWICH CONSTRUCTION

FIG. 1



SCHEMATIC OF
HONEYCOMB SANDWICH BEAM

FIG. 2



HONEYCOMB CORE

FIG. 3

2. Experimental Methods

There are various methods of specifying the amount of damping that exists in an engineering material, two of which are outlined in the introduction: the resonant amplification factor and the logarithmic decrement. These two methods are related to two experimental methods of observing the damping behavior: the steady state forced vibration method and the transient, or free vibration decay, method. Both experimental methods are used in this project.

The steady state forced vibration test method basically consists of establishing the resonance vibration curve, i.e., the amplification factor over a range of frequencies including the resonant frequency. The amplification factor of a cantilever beam may be expressed as the ratio of the amplitude y_0 at the tip of the beam to the amplitude a_0 at the root of the beam when the root has a forced harmonic motion. Thus [3]:

$$A = y_0/a_0 \quad (6)$$

From an engineering viewpoint, the maximum value of the amplification factor and the frequency at which this occurs are of major interest. The resonant amplification factor can be determined experimentally as the maximum value of the amplification factor or peak of the resonance curve of a steady state forced vibrating cantilever beam [3]:

$$A_r = (y_0/a_0)_{\max} \quad (7)$$

The steady state forced vibration test method has the capability of obtaining damping information over a spectrum of frequencies in addition to affording simplicity in computing damping effectiveness. In this study only the fundamental frequency is examined. The basic

equipment requirements are:

- a. Vibration generator capable of producing vibrations over a useful frequency range;
- b. Accurate means of measuring frequency of vibrations;
- c. Equipment for measuring vibration amplitudes.

An electromagnetic shaker is employed as a vibration exciter. The shaker is powered by a low distortion power amplifier with a variable frequency sine wave generator as a signal source.

In determining the resonance curve, the tip amplitude and root amplitude of the beam, plus the vibration frequency, must be measured. An accelerometer in conjunction with a cathode follower and vacuum tube voltmeter (VTVM) is used to measure the amplitude at the root of the beam. A microscope is used to measure the tip amplitudes. The frequency of vibration is measured by an electronic counter.

The specimen beams are mounted on a spindle which is an extension of the vibration generator. This is accomplished by an aluminum disc with a threaded central hole which is bonded to the lower surface of the specimen beam at mid-length and screwed onto the spindle.

Prior to testing, all electronic instruments are turned on and warmed up in accordance with manufacturers' instructions and the ambient level on the VTVM recorded. The microscope is calibrated and focused on a scribe line on the end of the beam. The thickness of the scribe line is recorded to deduct from amplitude measurements when the beam is vibrating. Forced vibrations are initiated and the sine wave is checked over the range of frequencies intended for testing to insure no distortion. The resonant frequency is then found and the forced

vibration set, such that the peak to peak end amplitude is approximately five divisions on the microscope scale. Observations are then made over a two cycle band width, centered at the resonant frequency, at intervals of approximately 0.1 cps. After returning to the resonant frequency, the amplitude of the forced vibrations is varied over a suitable range, up to the limits of the vibration generator, to observe the variation of damping with amplitude of vibration.

The free vibration decay test method basically consists of initiating free vibrations in the cantilever beam and measuring the frequency and rate of decay of the free vibrations, or the logarithmic decrement as expressed in equation (4).

The method of mounting the specimen beams in this test method is the same as in the steady state forced vibration test method except that the mounting spindle is attached to a rigid foundation. The means used to initiate free vibrations is a five pound weight suspended from the ends of the center-mounted beam by 0.001" diameter iron wire. A spreader is used to keep the deflecting force on the beam vertical. Strain energy is stored in the beam and free vibrations begin when the wire is melted, suddenly releasing the weight. The vibration amplitude decays until the strain energy is dissipated. Four foil resistance type strain gages, arranged in a four gage bridge, are used on each beam to sense the vibration through cyclic variation of strains in the material. The strain gage signal is amplified, then recorded by an oscillograph with fluid type galvanometers and a companion timing unit.

Prior to testing, the galvanometer heating circuit is turned on and the fluid type galvanometers warmed up. The amplifier is warmed

up in accordance with manufacturer's instructions. The bridge is balanced with no load on the beam, after which the beam is loaded and the gain selected for maximum initial amplitude of vibration. The load is then removed from the beam and the trace calibrated. The beam is loaded by looping mild steel wire through two eye-bolts in a block, which supports the five pound weight. The ends of the wire are looped around the two ends of the beam and a spreader used to keep the wire running vertically down from the ends of the beam. A plumb bob is used to position the five pound weight under the center of the beam. After starting the oscillograph at the desired speed (25 in./sec) the weight is released by melting the wire between the two eye-bolts with a propane torch.

There are six specimen beams tested by both the steady state forced vibration method and free vibration decay method. Five of the beams are of a length to thickness ratio of 20 and core thickness to total thickness ratios of approximately 0, 0.26, 0.40, 0.52 and 0.80. The sixth beam has a length to thickness ratio of 27.5 and a core thickness to total thickness ratio of approximately 0.26. The purpose of the solid beam is to determine experimentally a value of the damping constant J which is employed in equations (26) and (28) of Appendix I to predict the resonant amplification factor A_r for the honeycomb sandwich beams.

3. Experimental Results

Experimental results are summarized on pages 14 to 17. The experimental results of the steady state forced vibration test method are presented on graphs, Figs. 4 and 5. Results are also listed in Tables I and III for comparison with predicted values. The experimental results of the free vibration decay test method are listed in Tables II and III.

The results of the steady state forced vibration tests in Fig. 4 show the variation of the resonant amplification factor versus tip amplitude of the beam. The initial portion of several of the curves is dashed because the ambient voltage on the voltmeter, used in determining the root amplitude, is approximately ten per cent of the recorded amplitudes. This lends some uncertainty to the reliability of the resonant amplification factor in this portion of the curve. As the root amplitude increases, the effect of the ambient voltage becomes much less and the trend of the curves becomes more evident.

The curves in Fig. 4 indicate a decrease of the resonant amplification factor as the tip amplitude of the beam increases in all cases except for the longer beam. The slope of the curves is an indication of the value of the damping exponent n . The damping exponent is evaluated in Appendix III from each of the curves in Fig. 4 and the results are listed in Table I.

In Table I the resonant amplification factor as found experimentally by the steady state forced vibration test method is compared with predicted values for damping exponents of two and three. The experimental values are taken from Fig. 4 for a tip amplitude of 0.008". The

predicted values were computed using the same amplitude. Comparison of the observed resonant amplification factor with that predicted reveals the erratic behavior of the observed values. This behavior suggests the influence of damping other than that of the beam itself. The bonding material between the bottom face of the beam and the aluminum mounting disc is believed to have contributed a major portion of this damping energy. The damping characteristics of the bonding material, Eastman 910 adhesive, are beyond the scope of this project. However, an analysis is made in Appendix III to approximate the magnitude of the strain energy involved. The results indicate the strain energy in the bond may be of the order of magnitude of 40 per cent of the total strain energy in the beam. The curves of Fig. 5 are the results of an attempt to evaluate the damping influence of the bonding material between the beam and the aluminum disc. The lower curve gives the results of a test in which the solid beam was partially drilled and tapped, as indicated in Fig. 5, as a means of mounting the beam. These results are very nearly coincident with the results of the tests with the bonded aluminum disc mounting system.

The results of the resonant amplification factor as observed by the free vibration decay tests are listed in Table II for average tip amplitudes. These results also show erratic behavior for the various core thicknesses. Comparisons with Fig. 4 also indicate resonant amplification factors much less than the results of the steady state forced vibration test method. This suggests the influence of additional damping other than from the beam itself and the mounting system. There are several places suspected where this energy is being

dissipated. The segments of wire which remain attached to the ends of the beam after melting to release the five pound weight are suspected of contributing the major portion of this stray damping. The other mechanisms suspected of dissipating energy are the foil strain gages, their bonding material, and short segments of electrical connections from the gages to the point where the leads are secured to the mounting spindle.

The results of resonant frequency measurements of both test methods are compared with predicted values in Table III. Two predicted frequencies are listed, the column headed by "w/shear" takes into account the effect of shear in the core, while the column headed by "w/o shear" completely neglects the effect of shear in the core. The computations for the two predicted frequencies are illustrated in Appendix III. Examination of Table III reveals close agreement between the observed resonant frequencies of the test methods. Comparison of the observed with the predicted resonant frequencies shows agreement within six per cent between the observed and the predicted values, neglecting the effect of shear in the core for the six beams.

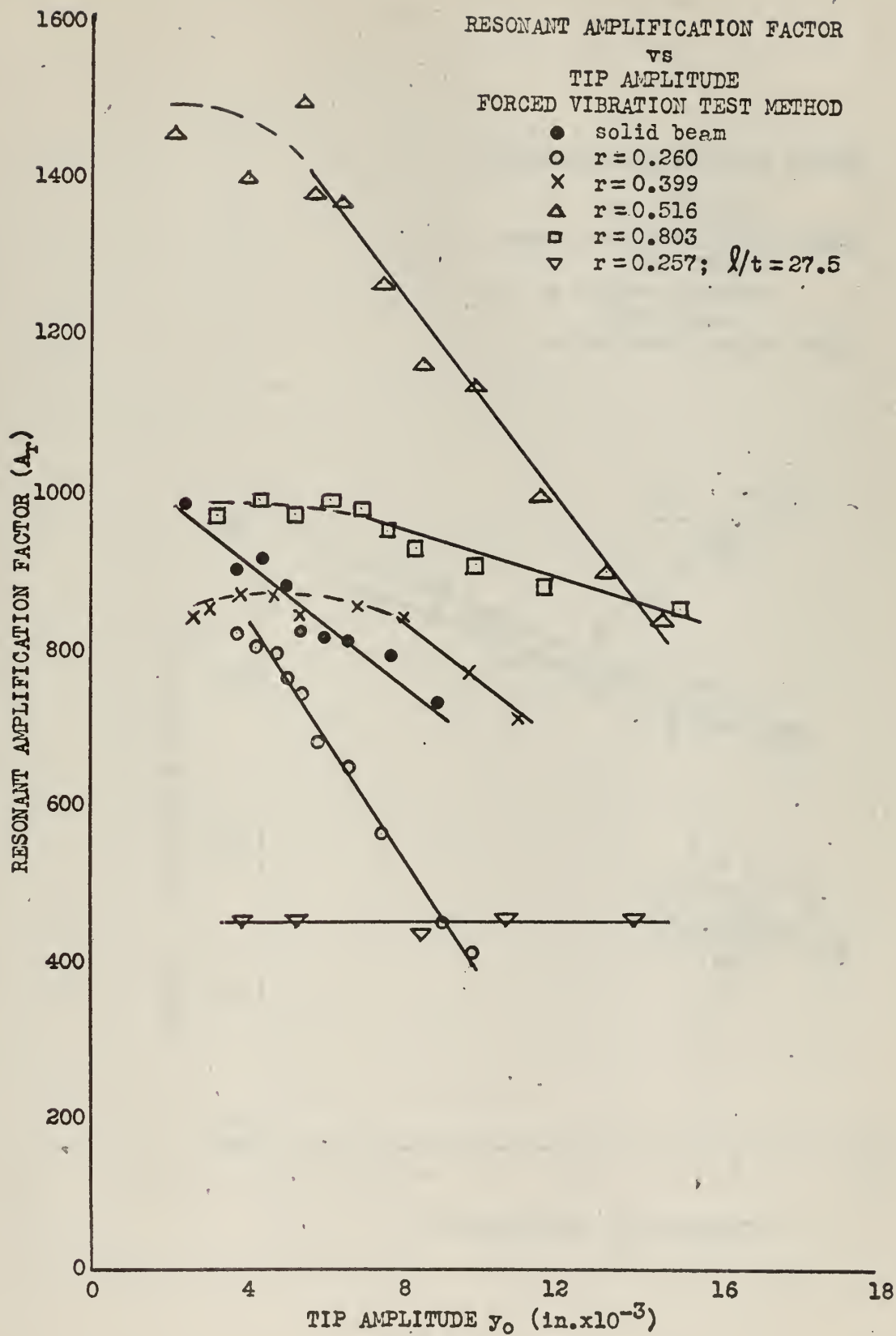


FIG. 4

RESONANT AMPLIFICATION FACTOR
 vs
 TIP AMPLITUDE
 FORCED VIBRATION TEST METHOD
 SOLID BEAM

- bonded aluminum disc mtg.
- drilled & tapped mtg.

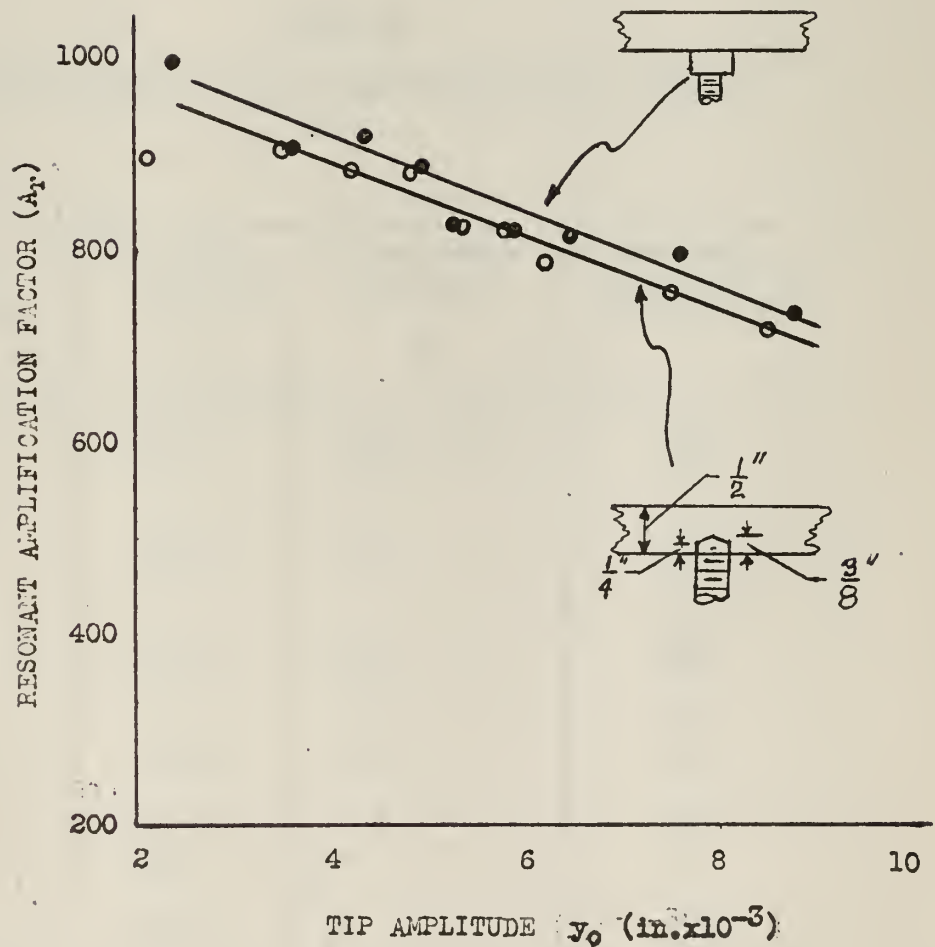


FIG. 5

TABLE I

DAMPING RESULTS FROM STEADY STATE FORCED VIBRATION TEST

$$(y_0 = 0.008 \text{ in.})$$

$r = t_c/t$	Observed	Predicted		n (obs.)
	A_r	A_r n = 3	A_r n = 2	
0	760	760	760	2.28
0.260	520	580	715	2.82
0.399	820	605	715	2.45
0.516	1260	660	715	2.63
0.803	960	1250	715	2.21
0.257 $l/t = 27.5$	445	1150	725	2.00

TABLE II

DAMPING RESULTS FROM FREE VIBRATION DECAY TESTS

$r = t_c/t$	Tip Amplitude y_0 10^{-3} in.	Logarithmic Decrement δ	Resonant Amplification Factor A_r
0	3.82	6.5×10^{-3}	490
	6.84	6.9 "	450
0.260	4.06	7.8 "	400
	5.98	9.3 "	340
0.39	3.82	5.1 "	620
	7.72	5.4 "	590
0.516	3.18	7.5 "	420
	7.56	8.7 "	370
0.803	4.64	8.5 "	380
	12.6	12. "	270
0.257 $l/t = 27.5$	7.52	18. "	300
	19.5	19. "	290

TABLE III
COMBINED RESONANT FREQUENCY RESULTS

$r = \frac{t_c}{t}$	Observed		Predicted	
	Free Vibration Test cps	Resonance Curve cps	w/shear cps	w/o shear cps
0	166.3	166.0	163.2	163.2
0.260	179.7	181.7	155.3	132.0
0.399	192.0	192.4	163.8	198.5
0.516	194.3	195.5	171.5	207.0
0.803	224.2	225.3	197.0	226.0
0.257 $\lambda/t = 27.5$	96.2	95.9	89.6	95.6

4. Conclusions

From the results of the study of the damping characteristics of honeycomb sandwich construction, the following conclusions can be drawn.

The damping capacity of the honeycomb sandwich beam as specified by the resonant amplification factor is dependent on the stress level for four of the five honeycomb sandwich beams tested. This is indicated by the decrease in the resonant amplification factor for an increase in the tip amplitude of the beams. The damping exponent n , which indicates the degree to which the damping energy is dependent on the stress level, is determined to be between two and three for the honeycomb sandwich beams tested. The evaluation of the damping exponent n and the order of magnitude of the damping constant J found experimentally from the solid beam agree with values of these constants for most engineering materials [1], [2], [7].

The mounting system used in the test methods employed in this study contributed considerable additional damping in relation to the damping of the beams tested. The effect of stray damping limits the conclusions which can be made in comparing theory with test results for the variation of amplification factor for increased core thickness. The initial introduction of the core into the beam has the greatest effect in increasing damping as indicated by a decrease in the resonant amplification factor. As the ratio of core thickness to total beam thickness is increased, although the results are erratic, indications are that the damping decreases.

The fundamental frequency of vibration of the honeycomb sandwich beams studied may be predicted within six per cent, using the conventional Rayleigh method and neglecting the effect of shear in the core.

BIBLIOGRAPHY

1. J. E. Ruzicka, New Design Techniques for Damping Structural Resonance, Barry Controls Inc., Watertown, Massachusetts.
2. J. E. Ruzicka, (editor), Structural Damping, ASME, New York, 1959.
3. B. J. Lazan, Effect of Damping Constants and Stress Distribution on the Resonance Response of Members, J. Appl. Mech., Vol.20, pp 201-209, 1953.
4. A. L. Kimball and D. E. Lovell, Internal Friction in Solids, Phys. Review, Second Series, Vol.30, pp 948-959, 1927.
5. B. J. Lazan, Mechanical Properties of Plastics and Metals Under Sustained Vibrations, ASME Trans., Vol.65, 1943.
6. J. H. Klumpp and B. J. Lazan, Frictional Damping and Resonant Vibration Characteristics of an Axial Slip Lap Joint, WADC Tech. Rpt. pp 54-64, March, 1954.
7. J. M. Robertson and A. J. Yorgiadis, Internal Friction in Engineering Materials, J. Appl. Mech., Vol.13, pp A173-182, 1946.
8. S. Timoshenko and J. N. Goodier, Theory of Elasticity, Second Ed., Mc Graw-Hill Co., 1951.
9. J. P. Den Hartog, Mechanical Vibrations, Fourth Ed., Mc Graw-Hill Co., 1956.
10. Endevco, Instructions for 2110 Impedance Head, Endevco Corp., Pasadena, California, Rev. 1961.

APPENDIX I

THEORETICAL ANALYSIS

The resonant amplification factor A_r is the primary method selected to specify the amount of damping that exists in sandwich construction material. From equation (1) page 2:

$$A_r = \frac{2\pi U_o}{D_o} \quad (1)$$

The damping energy and the strain energy in sandwich construction are composed of two parts. Assuming rigid attachment of the core to the facings, these are the energy in the core and the energy in the facings. It is also assumed that the strain energy due to shear in the facings is negligible compared to the energy due to bending and that the energy due to bending in the core is negligible compared to the energy due to shear. The strain energy and damping energy are:

$$U_o = U_b + U_s$$

$$D_o = D_{ob} + D_{os}$$

where the subscript b refers to the bending energy in the facings and s refers to the shear energy in the core.

The definitions of these energy terms follow from the principles of basic strength of materials. The strain energy due to bending (in the facings) is:

$$U_b = \frac{1}{2} \int_0^l \frac{M_x^2}{E_x I_x} dx \quad (8)$$

where, at any point x along the beam:

M_x = bending moment

E_x = modulus of elasticity

I_x = centroidal moment of inertia of section area

l = length of beam

The strain energy due to shear in the core is

$$U_s = \int_0^l \int_{-\frac{t_c}{2}}^{\frac{t_c}{2}} w \frac{\tau_x^2}{2G} dy dx \quad (9)$$

where, at any point x along the beam:

τ_x = shear stress

G_x = shear modulus

w = width of beam

Two types of stress are assumed present in the honeycomb constructed beam: uniaxial stress in the facings; and pure shear in the core. It has been shown by previous investigation [7] that internal friction in engineering materials, as represented by the damping capacity, is due only to the distortion of the material. Thus for equal damping energies under uniaxial stress and under pure shear:

$$D = J_b \sigma^n = J_s \tau^n$$

and for equal distortion energies [8]:

$$\frac{\tau}{\sigma} = K = \frac{1}{\sqrt{3}}$$

therefore

$$J_s = J_b / K^n \quad (10)$$

The damping energy due to bending in the facings is [3]

$$D_{ob} = \iint D_b w dx dy$$

where the specific damping energy is

$$D_b = J_b \sigma^n$$

and

$$\sigma = \frac{y}{t/2} \sigma_x$$

where σ is the stress at any point, σ_x is the maximum stress (at the outer fibers) at any position x along the length of the beam, and $t/2$ is the maximum distance from the neutral axis to the outer fibers at x . Therefore:

$$D_{ob} = \int_0^l \int_{-\frac{t_c}{2}}^{\frac{t_c}{2}} w J_b \left(\frac{y}{t/2} \right)^n \sigma_x^n dy dx \quad (11)$$

The damping energy due to shear in the core is

$$D_{os} = \iint D_s w dy dx$$

where the specific damping energy is

$$D_s = J_s \tau^n$$

Substituting equation (10) gives

$$D_{os} = \int_0^l \int_{-\frac{t_c}{2}}^{\frac{t_c}{2}} w J_b \left(\frac{\tau}{k} \right)^n dy dx \quad (12)$$

Substituting equations (8), (9), (11) and (12) into equation (1),

the resonant amplification factor becomes

$$A_r = \frac{2\pi}{J_b} \left[\frac{\frac{1}{2} \int_0^l \frac{M_x^2}{E_x I_x} dx + \int_0^l \int_{-\frac{t_c}{2}}^{\frac{t_c}{2}} w \frac{\tau_x^2}{2G} dy dx}{2 \int_0^l \left[\int_{-\frac{t_c}{2}}^{\frac{t_c}{2}} w \left(\frac{2y}{t} \right)^n dy \right] \sigma_x dx + \frac{1}{k^n} \int_0^l \int_{-\frac{t_c}{2}}^{\frac{t_c}{2}} w \tau_x^n dy dx} \right] \quad (13)$$

Equation (13) describes the damping characteristics of a honeycomb sandwich construction beam. This analysis is restricted to a symmetrical beam, i.e., the facings are of equal thickness, and the core and facings are of the same material.

For purposes of further analysis a symmetrical cantilever beam with constant cross section is assumed with core and facings of

aluminum alloy. The core is composed of a hexagonal honeycomb pattern suitably bonded to the facings. The value $n=3$ is assumed for room temperatures, moderate cyclic stress history, and stress levels considerably less than the yield strength.

Incorporating these assumptions into equation (13)

$$A_r = \frac{2\pi}{J_b} \left[\frac{\frac{1}{2EI} \int_0^l M_x^2 dx + \frac{t_c W}{2G} \int_0^l \tau_x^2 dx}{\frac{W}{4} \left(\frac{t^4 - t_c^4}{t^3} \right) \int_0^l \tau_x^3 dx + \frac{W t_c}{K^3} \int_0^l \tau_x dx} \right] \quad (14)$$

For a cantilever beam vibrating in its fundamental mode the extreme deflection is assumed to be represented by:

$$y = y_0 \left(1 - \cos \frac{\pi x}{2l} \right) \quad (15)$$

From basic strength of materials

$$M_x = \int_0^l (\xi - x) \mu \omega^2 y(\xi) d\xi$$

where ξ is a dummy variable, μ is the mass per unit length of the beam, and ω is the circular frequency. Then

$$M_x^2 = \mu^2 \omega^4 y_0^2 \left[\int_x^l (\xi - x) \left(1 - \cos \frac{\pi \xi}{2l} \right) d\xi \right]^2$$

Equation (8), representing the strain energy due to bending in the facings, becomes

$$U_b = \frac{1}{2EI} \int_0^l M_x^2 dx = 0.00918 \mu^2 \omega^4 \frac{y_0^2 l^5}{EI} \quad (16)$$

Similarly equation (11), representing the damping energy due to bending in the facings, can be evaluated. For

$$\sigma_x = \frac{M_x^{1/2}}{I}$$

then

$$\int_0^l \sigma_x^3 dx = \mu^3 \omega^6 y_0^3 \frac{t^3}{8 I^3} \int_0^l \left[\int_x^l (\xi - x) \left(1 - \cos \frac{\pi \xi}{2l} \right) d\xi \right]^3 dx$$

Then

$$D_{ob} = J_b \frac{w}{4} \left(\frac{t^4 - t_c^4}{t^3} \right) \int_0^l \sigma_x^3 dx = 0.000120 J_b w \frac{\mu^3 \omega^6 y_0^3 l^7}{I^3} (t^4 - t_c^4) \quad (17)$$

Before evaluating equations (9) and (12) to find the strain energy and damping energy due to shear in the core, the voids in the core must be considered. For calculating the shear stress, an equivalent width for the core gives the desired results. Referring to Fig. 3

$$W_c = \rho_c w t_c \lambda$$

where W_c is the weight of the core in a length λ , w is the beam width, and ρ_c is the specific weight of the honeycomb core. Also:

$$W_c = \rho_{al} t_c 2 w_e \lambda_i$$

where ρ_{al} is the specific weight of the honeycomb core alloy and

$$\lambda_i = \frac{\lambda}{1 + \cos \theta}$$

w_e = equivalent width of core for shear stress calculation
(2 w_i times the number of units in beam width w)

The equivalent width is

$$w_e = \frac{1}{2} w (1 + \cos \theta) \frac{\rho_c}{\rho_{al}}$$

Thus, for $\Theta = 60^\circ$

$$w_e = \frac{3}{4} \frac{\rho_c}{\rho_{al}} w \quad (18)$$

The presence of the voids also affects the volume summations in equations (9) and (12). Since τ_x does not vary with y , the voids are accounted for by taking

$$\int_{-\frac{t_c}{2}}^{\frac{t_c}{2}} w dy = \frac{\rho_c}{\rho_{al}} w t_c \quad (18a)$$

The shear stress in the core can be found from basic strength of materials

$$\tau = \frac{V_s Q_\tau}{I w_e}$$

where the shearing force V_s is

$$\begin{aligned} V_s &= \int_x^l \mu \omega^2 y dx = \mu \omega^2 y_0 \int_x^l \left(1 - \cos \frac{\pi x}{2l}\right) dx \\ &= \mu \omega^2 y_0 l \left[\left(1 - \frac{2}{\pi}\right) - \left(\frac{x}{l} - \frac{2}{\pi} \sin \frac{\pi x}{2l}\right) \right] \end{aligned}$$

and the first moment Q_τ of the facing area is

$$Q_\tau = \int_{\frac{t_c}{2}}^{\frac{t}{2}} y dA = \left(\frac{t+t_c}{2}\right) \left(\frac{t-t_c}{2}\right) w = w \frac{t^2 - t_c^2}{4}$$

Now, letting

$$\Lambda = \left[\left(1 - \frac{2}{\pi}\right) - \left(\frac{x}{l} - \frac{2}{\pi} \sin \frac{\pi x}{2l}\right) \right]$$

the shear stress becomes

$$\tau_x = \frac{\mu \omega^2 y_0 l w (t^2 - t_c^2)}{4 I w_e} \Lambda$$

Substituting the shear stress into equation (9), the strain energy due to shear in the core is:

$$U_s = \left(\frac{\rho_c w t_c}{\rho_{al} 2G} \right) \int_0^l \tau_x^2 dx = \frac{1}{18G} \cdot \frac{\mu^2 \omega^4 y_0^2 l^2}{I^2 (\rho_c / \rho_{al})} w t_c (t^2 - t_c^2)^2 \int_0^l \Lambda^2 dx \quad (19)$$

and the damping energy due to shear in the core, from equation (12) is:

$$D_{bs} = \frac{J_b \rho_c w t_c}{\rho_{al} K^3} \int_0^l \tau_x^3 dx = \frac{J_b}{27 K^3} \frac{\mu^3 \omega^6 y_0^3 l^3}{I^3 (\rho_c / \rho_{al})^2} w t_c (t^2 - t_c^2)^3 \int_0^l \Lambda^3 dx \quad (20)$$

Evaluating the integrals in equations (19) and (20) gives

$$\int_0^l \Lambda^2 dx = 0.0832 l$$

$$\int_0^l \Lambda^3 dx = 0.0271 l$$

Substituting equations (16), (17), (19) and (20) into equation (14), the resonant amplification factor A_r for a symmetrical cantilever beam of honeycomb sandwich construction becomes

$$A_r = \frac{2\pi}{J_b} \left[\frac{0.00918 \frac{\mu^2 \omega^4 y_0^2 l^5}{EI} + 0.00462 \frac{\mu^2 \omega^4 y_0^2 l^3}{GI^2 (\rho_c / \rho_{al})} t_c (t^2 - t_c^2)^2}{0.000120 \frac{\mu^3 \omega^6 y_0^3 l^7}{I^3} (t^4 - t_c^4) + \frac{0.00100}{K^3} \frac{\mu^3 \omega^6 y_0^3 l^4}{I^3 (\rho_c / \rho_{al})^2} t_c (t^2 - t_c^2)^3} \right] \quad (21)$$

Rearranging and substituting $I = \frac{w(t^3 - t_c^3)}{12}$

$$A_r = \frac{2\pi K^3 I}{J_b G \mu \omega^2 y_0 l t^2} \cdot \frac{\rho_c}{\rho_{al}} \left[\frac{0.166 \frac{G}{E} \frac{\rho_c}{\rho_{al}} \left(\frac{l}{t} \right)^2 \frac{1-r^3}{(1-r^2)^2} + r}{0.0231 \left(\frac{\rho_c}{\rho_{al}} \right)^2 \left(\frac{l}{t} \right)^3 \frac{1+r^2}{1-r^2} + r(1-r^2)} \right] \quad (22)$$

where $r = \frac{t_c}{t}$ is the ratio of core thickness to total thickness.

Before deriving the resonant amplification factor in its final form, the frequency must be evaluated for substitution into equation (22). The frequency can be found using Rayleigh's method [9].

$$\text{Maximum Strain Energy} = \text{Maximum Kinetic Energy}$$

or

$$U_b + U_s = T \quad (23)$$

The parts of the strain energy U_b and U_s have been determined in equations (16) and (19). The maximum kinetic energy

$$T = \frac{1}{2} \int \dot{w}^2 dm = \frac{1}{2} \mu \omega^2 \int_0^l y^2 dx$$

where y is given by equation (10). Thus:

$$T = 0.1134 (\mu \omega^2 y_0 l) \quad (24)$$

Substituting equations (16), (19) and (24) into equation (23) and solving for ω^2 gives

$$\omega^2 = (3.52)^2 \left[\frac{EI}{\mu l^4} \right] \left[\frac{1}{1 + \beta} \right] \quad (25)$$

where

$$\beta = 6.03 \frac{E}{G} \frac{\rho_c}{\rho_{al}} \left(\frac{l}{t} \right)^2 r \frac{(1-r^2)^2}{1-r^3}$$

Notice that for zero core thickness equation (25) reduces to that for a solid cantilever beam [9].

Substituting equation (25) into equation (22):

$$A_r = \frac{0.462}{J_b G E} \frac{\rho_c}{\rho_{al}} \frac{l}{y_0} \left(\frac{l}{t} \right)^2 \left[1 + \beta \right] \left[\frac{0.166 \frac{G}{E} \frac{\rho_c}{\rho_{al}} \left(\frac{l}{t} \right)^2 \frac{1-r^3}{(1-r^2)^2} + r}{0.0231 \left(\frac{\rho_c}{\rho_{al}} \right)^2 \left(\frac{l}{t} \right)^3 \frac{1+r^3}{1-r^2} + r(1-r^2)} \right] \quad (26)$$

Equation (26) is based on the assumption that the damping exponent $n = 3$. If $n = 2$ instead, equation (13) becomes

$$A_r = \frac{2\pi}{J_b} \left[\frac{\frac{1}{2EI} \int_0^l M_x^2 dx + \frac{t_c w}{2G} \int_0^l \tau_x^2 dx}{\frac{w}{3} \left(\frac{t^3 - t_c^3}{t^2} \right) \int_0^l \sigma_x^2 dx + \frac{w t_c}{K^2} \int_0^l \tau_x^2 dx} \right] \quad (27)$$

Substituting the previously evaluated integrals and arranging in dimensionless form:

$$A_r = \frac{\pi}{J_b E} \left[\frac{1 + 6.03 \frac{E}{G} \frac{\rho_{al}}{\rho_c} \left(\frac{t}{l} \right)^2 r \frac{(1-r^2)^2}{1-r^3}}{1 + 18.1 \frac{\rho_{al}}{\rho_c} \left(\frac{t}{l} \right)^2 r \frac{(1-r^2)^2}{1-r^3}} \right] \quad (28)$$

The damping, as specified by the resonant amplification factor, is constant for variations in cross section for a damping exponent $n = 2$ [3]. In equation (28) the resonant amplification factor will be constant for variations in r if, and only if, $E/G = 3$. In this project $E/G \neq 3$ and the term in the brackets is very nearly constant for all values of r except $r = 0$.

APPENDIX II

EXPERIMENTAL APPARATUS AND PROCEDURE

Basic Apparatus

The basic experimental apparatus consisted of five 20" beams and one 27.5" beam as illustrated in Fig. 6. The nominal dimensions of the beams were one inch in width and one-half inch in thickness. The beam dimensions are listed in Table V of Appendix IV. The honeycomb core material was made of 3003 aluminum base alloy with Hexcel core designation 3/16 .0018P 3003 and the facings of the honeycomb sandwich beams were made of 6061-T6 aluminum base alloy. The facings were bonded to the core using a Shell Epon 907 adhesive bonding material. The solid beam was made from 24S-T6

The beams were mounted on a spindle in both test methods used as illustrated in Figs. 7 and 8. An aluminum disc one inch in diameter and approximately one-half inch thick was bonded to the center of each beam with Eastman 910 adhesive. The aluminum discs were threaded to screw onto a mounting spindle. The aluminum disc was locked in place with a lock-nut, allowing no lost motion between the beam and the mounting spindle. In the steady state forced vibration test method, the spindle was an extension of the impedance head. In the free vibration decay test method, the spindle was mounted on a rigid support.

Instrumentation

In the steady state forced vibration test method, the equipment is illustrated in Fig. 7 and the schematic diagram below includes:

Vibration Generator

Goodman Ind. LTD.
Vibration Generator
Model 39A
Serial No. 417

Amplifier

Krohn-Hite Inst. Co.
Ultra-low Distortion Power
Amplifier Model UF-101
Serial No. 135

Signal Generator

Donner Scientific Co.
Sine Wave Generator
Donner Model 1202
Serial No. 224

Accelerometer

Endevco Corp.
Model 2110 Impedance Head
Serial No. DA22

Cathode Follower

Endevco Corp.
Cathode Follower
Drawing No. X01066

Voltmeter

Hewlett Packard Model 400D
Vacuum Tube Voltmeter
Serial No. 22773

Electronic Counter

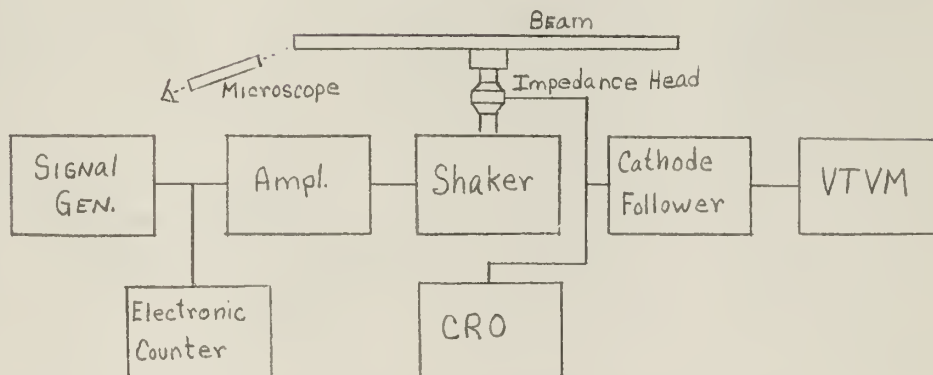
Eput Meter Model 554 S
Electronic Counter
Electro-Engineering Works
Serial No. E 6979

Oscilloscope

Hewlett Packard Model 130A
Cathode Ray Oscilloscope
Serial No. 2417

Microscope

Gaertner Reading Microscope

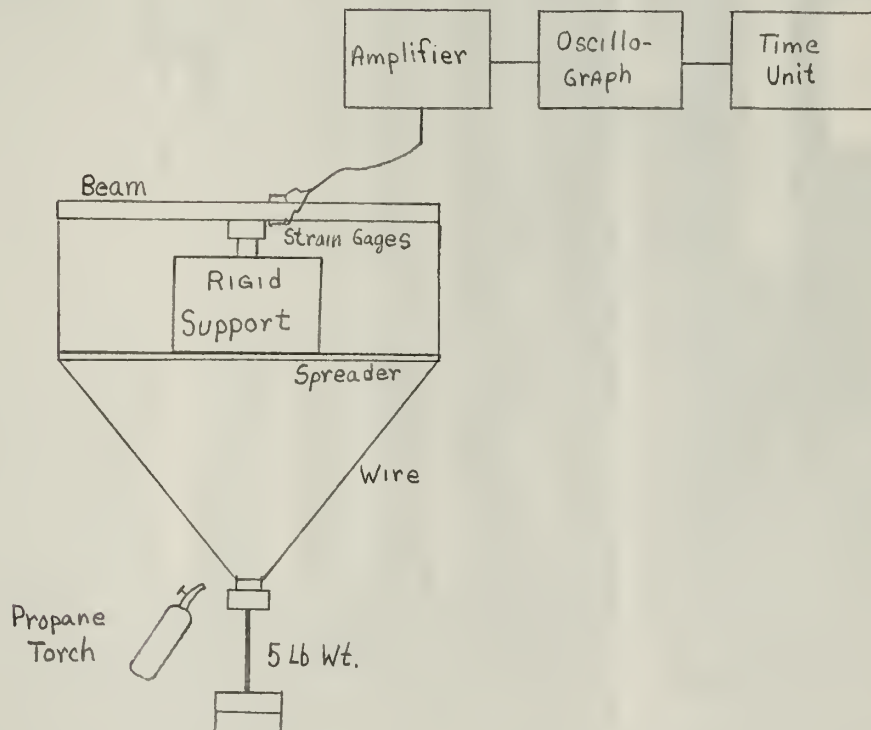


SCHEMATIC DIAGRAM OF FORCE VIBRATION TEST EQUIPMENT

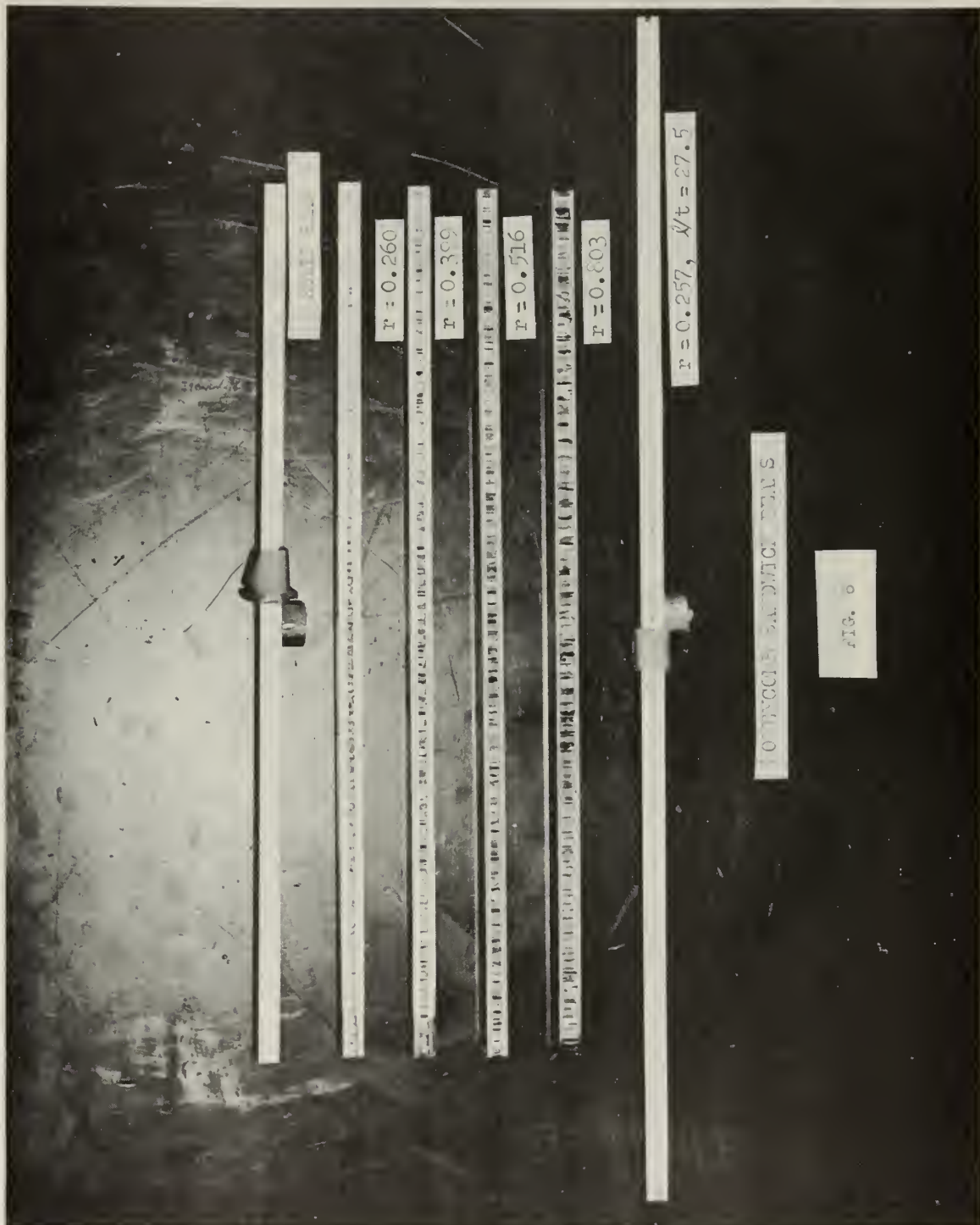
The following equipment was used in the free vibration decay test method as illustrated in Fig. 8 and in the schematic diagram below.

Vibration Source	Quick Release 5 lb weight
Strain Gages	Sr-4 FAP-12-12 Resistance Strain Gages
Amplifier	Honeywell Carrier Amplifier Model 130-2C Serial No. 130-162
Oscillograph	Honeywell Visicorder Model 906B with Series M1650 Fluid Damped Galvanometer Serial No. 9-7762
Timing Unit	Honeywell Timing Unit Serial No. 0725

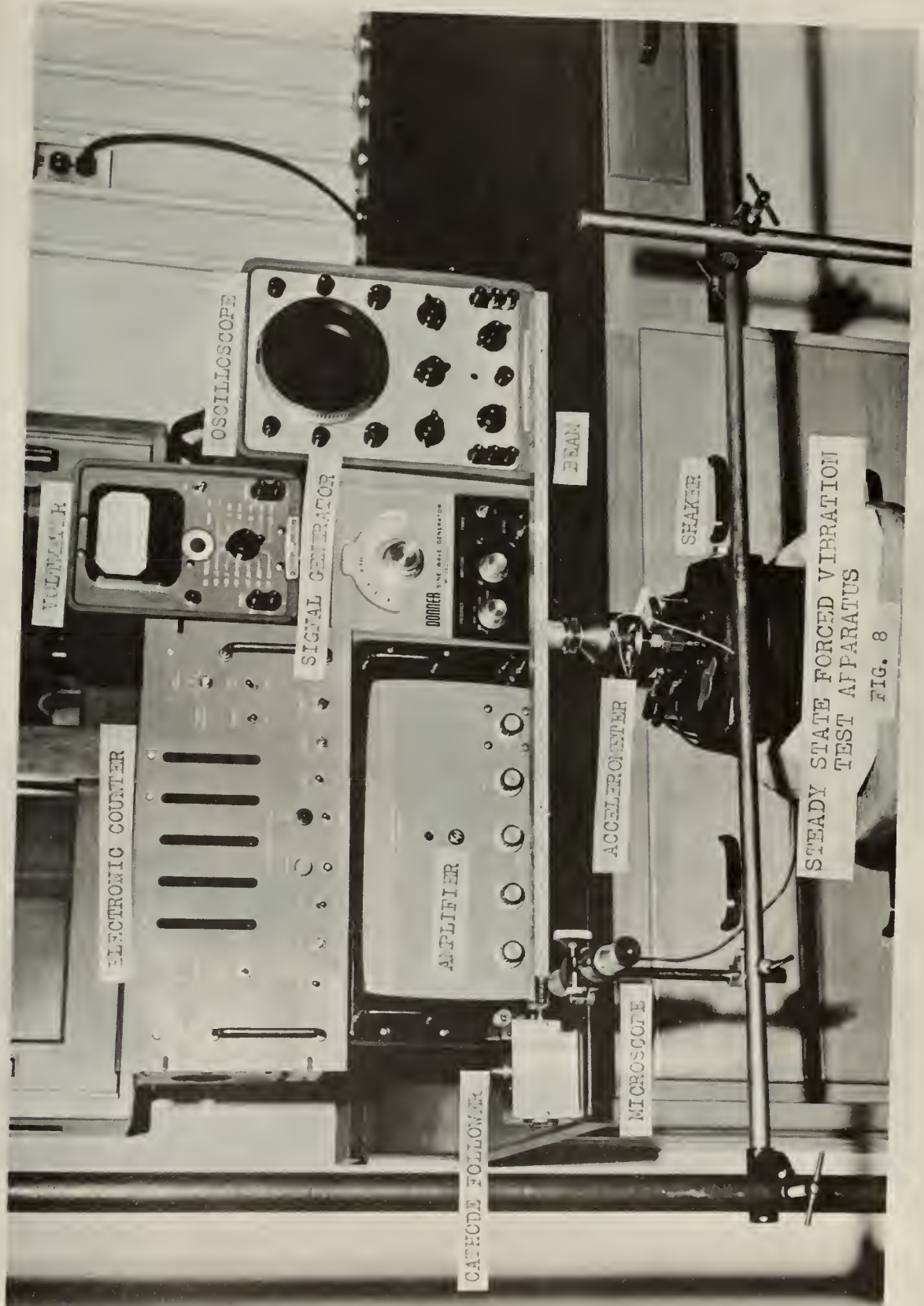
The strain gages were arranged in a four-gage bridge, two on the top and two on the bottom of each beam.

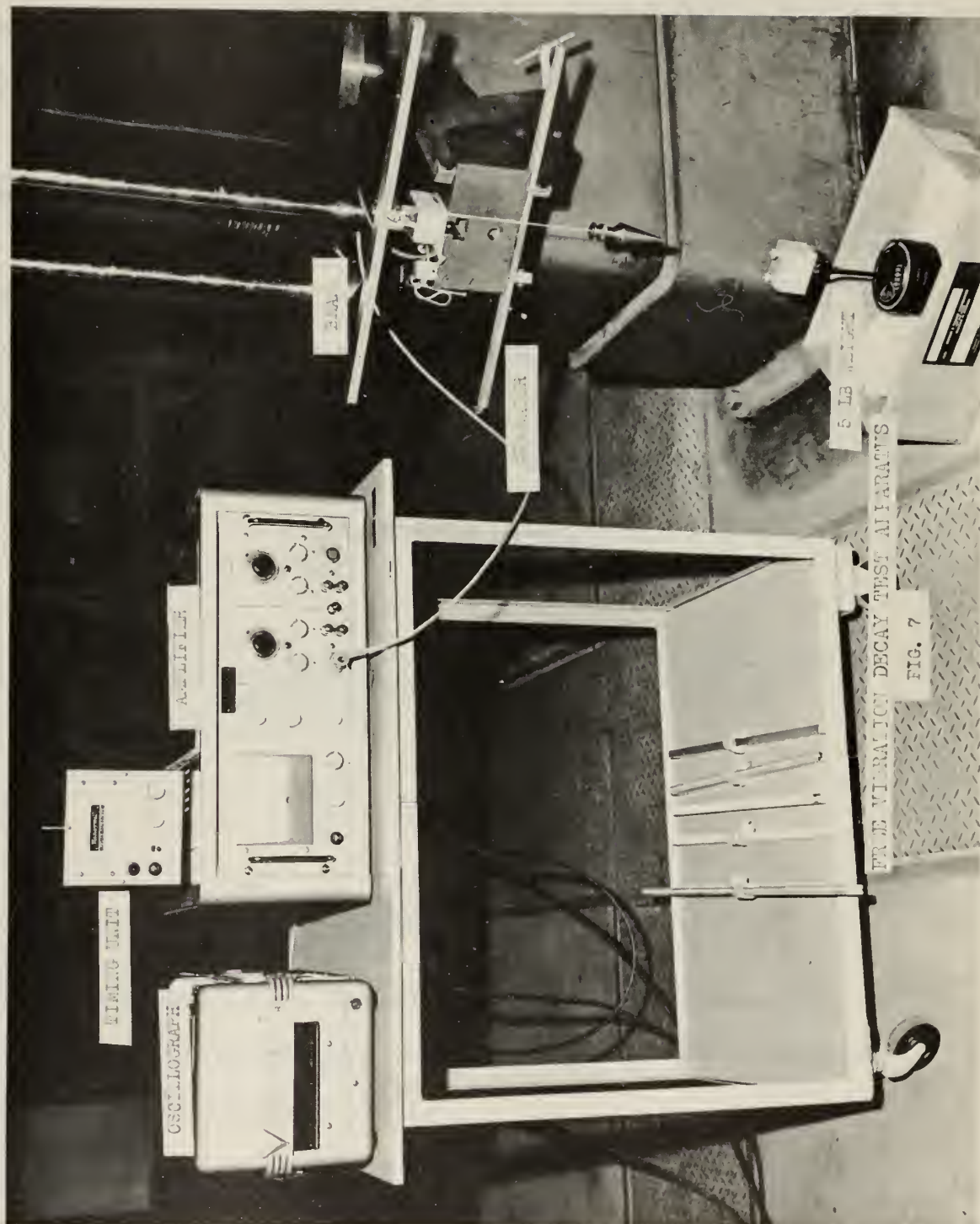


SCHEMATIC DIAGRAM OF FREE VIBRATION DECAY TEST EQUIPMENT









APPENDIX III

SAMPLE CALCULATIONS

The data on dimensions of all beams are listed in Table IV. These data were used in all calculations. In this Appendix, the data for the beam $r = 0.260$ is used for the sample calculations.

Predicted Resonant Amplification Factor

The equations for the predicted resonant amplification factors are developed in Appendix I, equations (26) and (28) for a damping exponent of three and two respectively. The damping constant J_b employed in these equations was found experimentally, using the resonant amplification factor for the solid beam. For the solid beam, equation (26) reduces to:

$$A_{r_{n=3}} = 3.31 \frac{l^2}{J_b E^2 y_0 t}$$

$$J_b = \frac{(3.31)(10^2)}{(760)(10.6 \times 10^4)^2 (.008)(0.5)} = 0.968 \times 10^{-12} \text{ psi}^{-2}$$

For the solid beam, equation (28) reduces to:

$$A_{r_{n=2}} = \frac{\pi}{J_b E}$$

$$J_b = \frac{\pi}{(760)(10.6 \times 10^6)} = 3.90 \times 10^{-10} \text{ psi}^{-1}$$

Listed in Table V are computed values for some dimensionless ratios used in the computations to follow. Equation (26) is repeated here for convenience.

TABLE IV
BEAM DIMENSIONS

$r = t_c/t$	t_f	t	t_c	l	w	W	l/t	ρ_c
—	inches					lbs	—	lb/ft ³
0	—	0.500	0	10.00	1.000	1.0030	20.00	—
0.260	0.186	0.503	0.131	10.01	1.002	0.7630	19.90	4.16
0.399	0.152	0.506	0.202	10.00	1.001	0.6240	19.77	4.40
0.516	0.120	0.496	0.256	10.01	1.002	0.4322	20.18	4.62
0.803	0.049	0.503	0.404	10.00	0.998	0.2426	19.89	4.48
0.257	0.186	0.501	0.129	13.76	1.002	1.0480	27.46	4.16

Solid Beam
 $E = 10.6 \times 10^6$ psi

Honeycomb Sandwich Beams
 $E = 10.0 \times 10^6$ psi
 $G = 3.87 \times 10^6$ psi

TABLE V
COMPUTED VALUES FOR HONEYCOMB BEAM
($r = 0.260$)

$r = t_c/t$	$1 - r^2$	$\frac{(1 - r^2)^2}{1 - r^3}$	$\frac{1 - r^3}{(1 - r^2)^2}$	$\frac{1 + r^2}{1 - r^2}$	$\frac{\rho_c}{\rho_{al}}$
0.260	0.932	0.885	1.130	1.137	0.024

$$A_{r, n=3} = \frac{0.462}{J_0 G E} \cdot \frac{\rho_c}{\rho_{al}} \cdot \frac{l}{y_0} \left(\frac{l}{t}\right)^2 [1 + \beta] \left[\frac{0.166 \frac{G}{E} \frac{\rho_c}{\rho_{al}} \left(\frac{l}{t}\right)^2 \frac{1-r^3}{(1-r^2)^2} + r}{0.231 \left(\frac{\rho_c}{\rho_{al}}\right)^2 \left(\frac{l}{t}\right)^3 \frac{1+r^2}{1-r^2} + r(1-r^2)} \right]$$

where:

$$\begin{aligned} \beta &= 6.03 \frac{E}{G} \frac{\rho_c}{\rho_{al}} \left(\frac{t}{l}\right)^2 r \frac{(1-r^2)^2}{1-r^3} \\ &= \frac{(6.03)(10^7)(0.503)^2(0.260)}{(3.87 \times 10^6)(0.0243)(10.01)^2} \cdot 0.885 = 0.374 \end{aligned}$$

The term outside the brackets becomes:

$$\frac{(0.462)(0.0243)(10.01)^3(1.374)}{(0.968 \times 10^{-12})(3.87 \times 10^6)(0.008)(0.503)^2} = 208$$

Within the brackets, the numerator is:

$$\frac{(0.166)(3.87 \times 10^6)(0.0243)(10.01)^2(1.130)}{(10 \times 10^6)(0.503)^2} + 0.260 = 0.966$$

and the denominator is:

$$\frac{(0.0231)(0.0243)(10.01)^3(1.137)}{(0.503)^3} + (0.260)(0.932) = 0.348$$

therefore

$$A_r = 208 \frac{0.966}{0.348} = 577$$

Equation (28) is also repeated:

$$A_{r_{n=2}} = \frac{\pi}{J_b E} \left[\frac{1 + 6.03 \frac{E}{G} \frac{\rho_{al}}{\rho_c} \left(\frac{t}{l}\right)^2 r \frac{(1-r^2)^2}{1-r^3}}{1 + 18.1 \frac{\rho_{al}}{\rho_c} \left(\frac{t}{l}\right)^2 r \frac{(1-r^2)^2}{1-r^3}} \right]$$

The term outside the brackets is the resonant amplification factor for the solid beam.

$$A_r = \frac{\pi}{J_b E} = 760$$

Within the brackets the numerator is:

$$1 + \frac{(6.03)(10^7)(0.503)^2(0.260)}{(3.87 \times 10^6)(0.0243)(10.01)^2} \times 0.885 = 1.374$$

and the denominator is:

$$1 + \frac{(18.1)(0.503)^2(0.260)}{(0.0243)(10.01)^2} \cdot (0.885) = 1.432$$

therefore

$$A_r = 760 \frac{1.374}{1.432} = 730$$

Predicted Frequencies

The equation for the resonant frequency, as derived in Appendix I, is equation (25):

$$\omega^2 = (3.52)^2 \left[\frac{EI}{\mu l^4} \right] \left[\frac{1}{1+\beta} \right] \quad (25)$$

or, in lb, in., sec units, the frequency f (cps) is

$$f = 4.496 \left[\frac{E_w}{Wl^3} \right]^{1/2} \left[t(1-r^3) \right]^{1/2} \left[\frac{1}{1+\beta} \right]^{1/2} \quad (25a)$$

where β was evaluated in the previous section.

$$f = 4.496 \left[\frac{(10^7)(0.503)^3(0.982)}{(0.763)(10.01)^3(1.374)} \right]^{1/2} = 155.3 \text{ cps}$$

Notice that the factor in equation (25) that contains β is due to the effect of shear in the core. If this term is set equal to zero this neglects the effect of shear in the core. Equation (25a) then becomes

$$f = 4.496 \left[\frac{E_w}{Wl^3} \right]^{1/2} \left[t(1-r^3) \right]^{1/2}$$

and

$$f = 4.496 \left[\frac{(10^7)(0.503)^3(0.982)}{(0.763)(10.01)^3} \right]^{1/2} = 182.0 \text{ cps}$$

Static Strain

From elementary strength of materials, the extreme fiber strain is:

$$\epsilon = \frac{M^{1/2}}{EI} = \frac{6}{E_w t^2} \left[\frac{Pl}{1-r^3} \right] = \frac{(6)(2.49)(9)}{(10^7)(0.503)^2(0.982)} = 55 \mu\text{in./in.}$$

Damping Exponent (n)

Equations (26) and (28) of Appendix I provide a means of evaluating the damping exponent n . For a value of two, there is no dependence of the resonant amplification factor on the tip amplitude of vibration. An inverse proportionality exists between the resonant amplification factor and the tip amplitude of vibration for a damping

exponent of three. Therefore, from equation (26) of Appendix I:

$$\frac{A_{r1}}{A_{r2}} = \left(\frac{y_{o2}}{y_{o1}} \right)^{n-2}$$

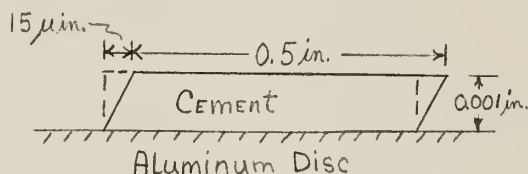
From Fig. 4, using the curve for $r = 0.260$

$$\frac{790}{410} = \left(\frac{9.7}{4.3} \right)^{n-2}$$

$$n = 2.82$$

Strain Energy in Mounting Bond

The strain energy in the bonding material between the aluminum disc and the lower face of the beam is considered to be due for the most part to the strain in beam. The thickness of the bond is estimated as 0.001" and the strain at the outer fiber of the beam is taken as 60 μ in./in.. A cross-section of the bonding material under the shear strain is shown in simplified form in the adjacent figure. The strain energy due to shear is:



$$U_a = \frac{\delta^2 A G}{2 h}$$

where:

δ = Average displacement (15 μ in.)

A = Area $\frac{\pi}{8}(D_o^2 - D_i^2) = 0.338 \text{ in.}^2$

h = 0.001 in.

G = Shear modulus of the bonding material - estimated as 100,000 psi

therefore

$$U_a = \frac{(15 \times 10^{-6})^2 (0.338) (10^5)}{(2) (0.001)} = 0.004 \text{ in.-lb}$$

Comparing this amount of strain energy with the total amount of strain energy in the beam with the suspended five pound weight prior to initiating vibrations in the free vibration decay tests:

$$W = \frac{1}{2} P y_0$$

$$W = \frac{1}{2} (2.5)(0.008) = 0.01 \text{ in.-lb}$$

The strain energy in the bonding material is approximately 40 per cent of the total strain energy in the beam.

APPENDIX IV

REDUCTION OF EXPERIMENTAL DATA

Forced Vibration Test Method

The measured data in the steady state forced vibration test method were the amplitudes at the tip and root of the beam and the frequency of vibration. The amplitude at the tip of the beam was measured in divisions of the scale marked on the reticle of the microscope. The microscope was calibrated with a standard calibration disc on which was etched a scale one centimeter in length with 100 divisions. Therefore, calibrating the microscope it was found

$$2.55 \text{ div. on microscope} = 0.01 \text{ cm}$$

Since the double amplitude of the tip of the beam was recorded, the amplitude y_0 is:

$$y_0 = \frac{\text{divisions on microscope}}{5.10 \times 2.54} \times 10^{-2}$$

$$y_0 = \frac{\text{div.}}{12.95} \times 10^{-2} \text{ in.}$$

The amplitude at the root of the beam was sensed by an accelerometer and displayed on the voltmeter in millivolts. The information taken from the manufacturer's instruction book on the Endevco 2110 Impedance Head, gives the acceleration in terms of the voltage output as [10]:

$$\text{acceleration} = \frac{V}{G_{CF}} \cdot \frac{1}{E_s} \left[\frac{C_p + C_t}{C_p + 100} \right]$$

thus

$$a_0 = \frac{1}{(2\pi f)^2} \cdot \frac{V}{G_{CF}} \cdot \frac{1}{E_s} \left[\frac{C_p + C_t}{C_p + 100} \right]$$

where

V - Voltage reading in millivolts on VTVM

G_{CF} - Gain of the cathode follower - - - - - 0.857

- E_s - Sensitivity of accelerometer - - - - - 51.5 $\frac{mv(rms)}{g \text{ pk}}$
 C_p - Capacitance of the accelerometer - - 1676 $\mu\mu f$
 C_t - Capacitance of the cathode follower
 and connector (12+97) - - - - - 109 $\mu\mu f$
 f - Frequency of vibrations in cps

Therefore the amplitude a_o of the root of the beam is

$$a_o = 0.223 \frac{V}{f^2} \text{ in.}$$

The frequency of vibrations was measured by an electronic counter set for a ten second counting period and displaying the frequency to the nearest 0.1 cps.

The resonance curves for the six specimen beams are shown in Figs. 9 to 11. The experimental data for the variation of the resonant amplification factor with tip amplitude are listed in Table VI and plotted in Fig. 4.

Free Vibration Decay Test Method

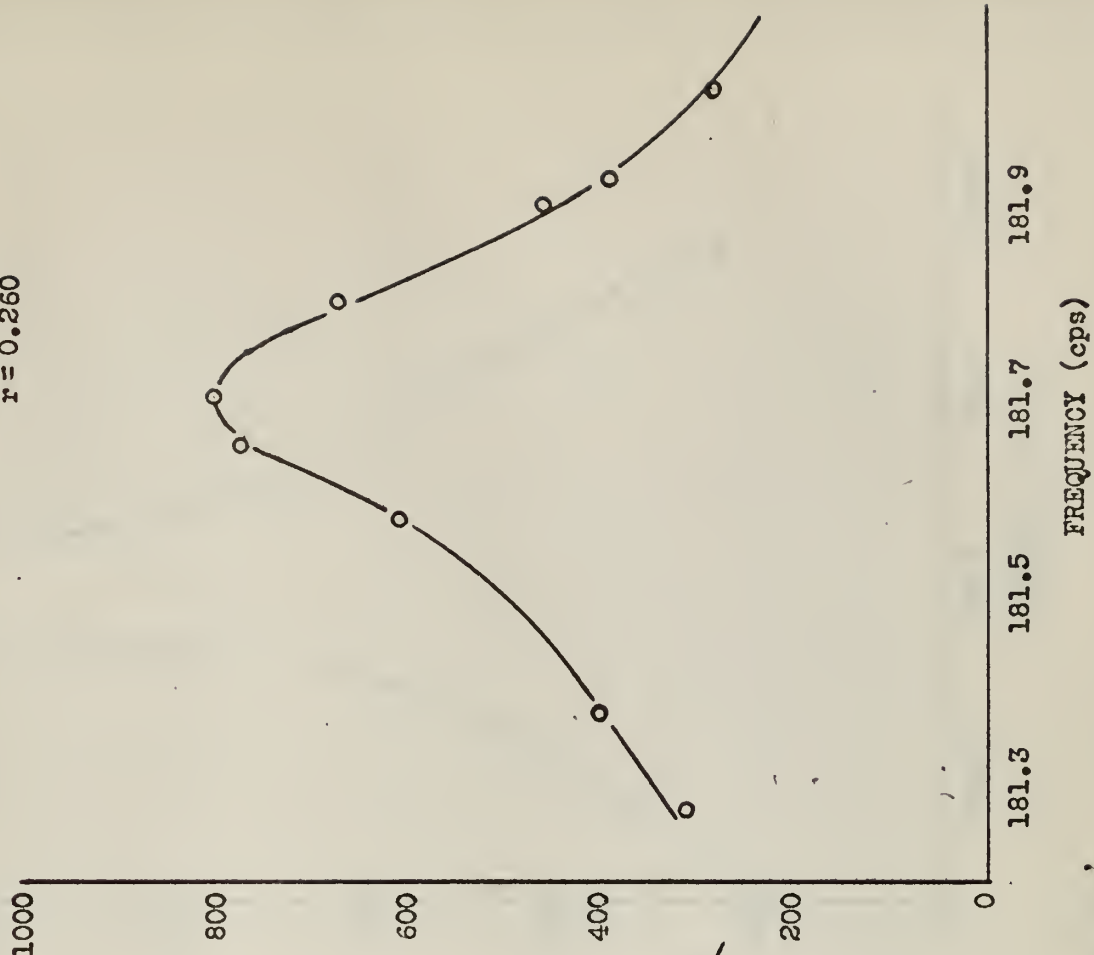
From the oscillograph record of free vibration decay, the data were reduced in the following manner: on each run, a zero time for amplitude measurements was selected. At this point, a short portion of the envelope of the vibration decay curve was determined by drawing the best straight line through two or three peaks on each side of the zero time. The measured zero amplitude X_o , was the distance between the envelope lines on the zero time line. Several more amplitudes (X_n , X_{2n} , X_{3n} - - -) were measured in the same manner at an elapsed time of n , $2n$, $3n$ - - - cycles, respectively, from zero time. A plot of the $\ln X$ vs n is a curve whose slope is equal to the logarithmic

decrement. The resultant curves showed slight curvature and thus were broken up into two parts for each run and the slope of each part determined for the logarithmic decrement. The data determined in this manner are listed in Table VII. The average of the three runs for both parts of the curve of each beam tested is listed in the results.

The frequency was determined by counting the number of cycles on the oscillograph record in a one second time period. This frequency for each of the three runs is listed in Table VII and the average is listed in the results.

A portion of an oscillograph record of the free vibration decay was copied and is shown in Fig. 12.

AMPLIFICATION FACTOR
vs
FREQUENCY
 $r = 0.260$



AMPLIFICATION FACTOR
vs
FREQUENCY
SOLID BEAM

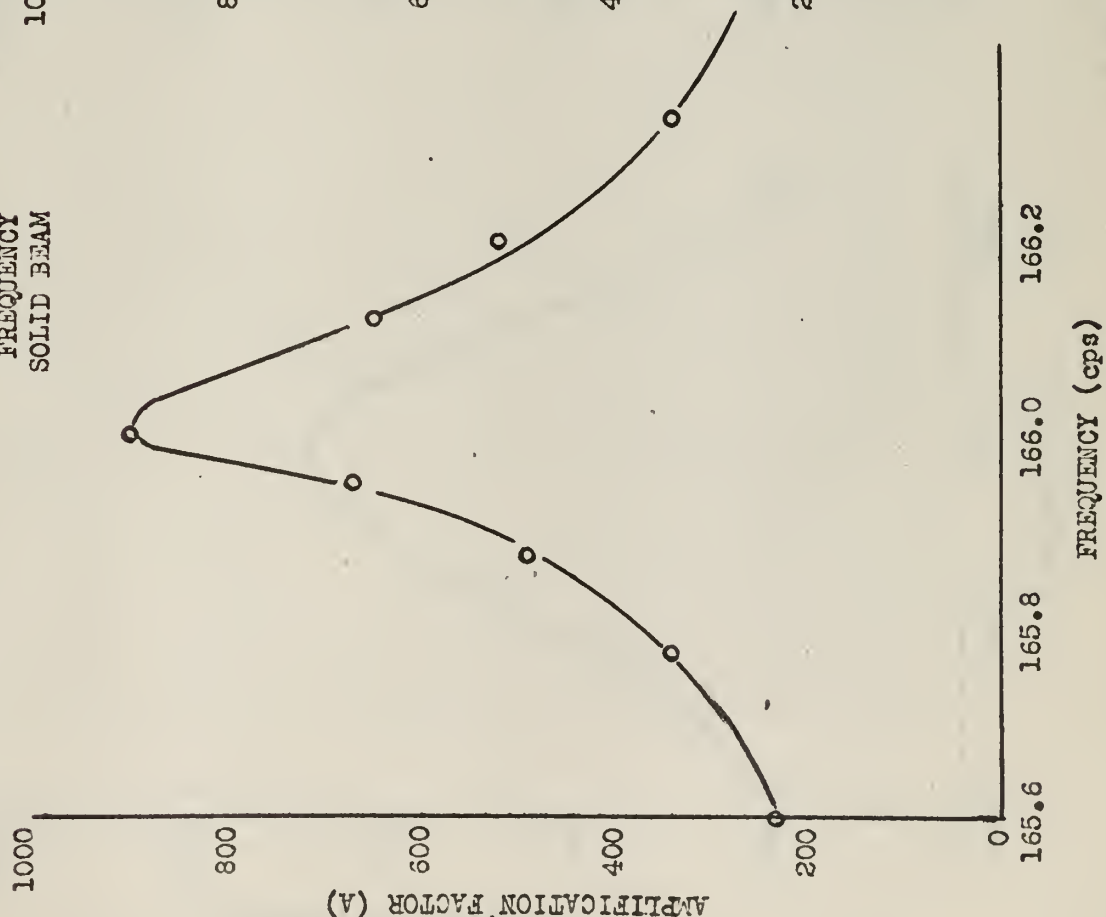


FIG. 9

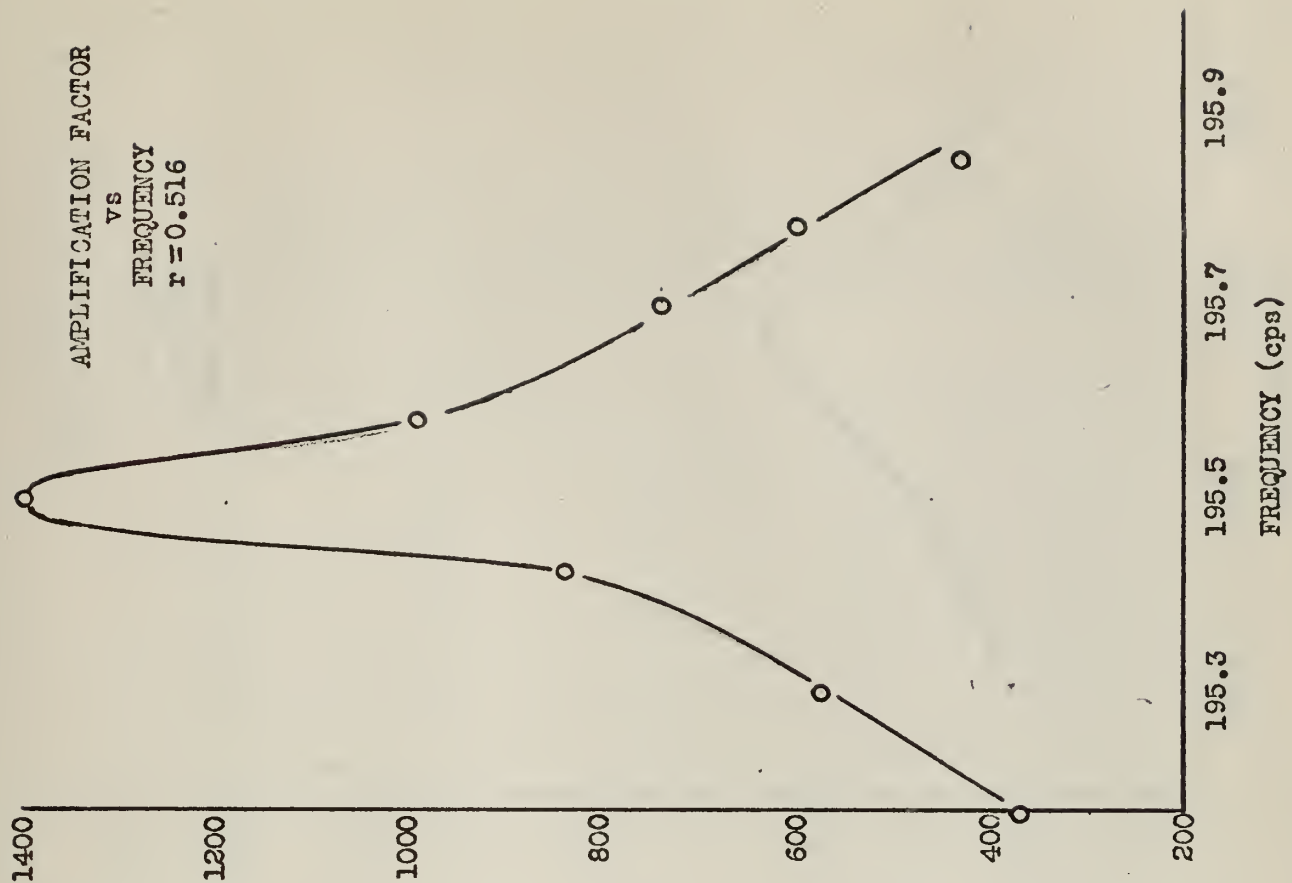
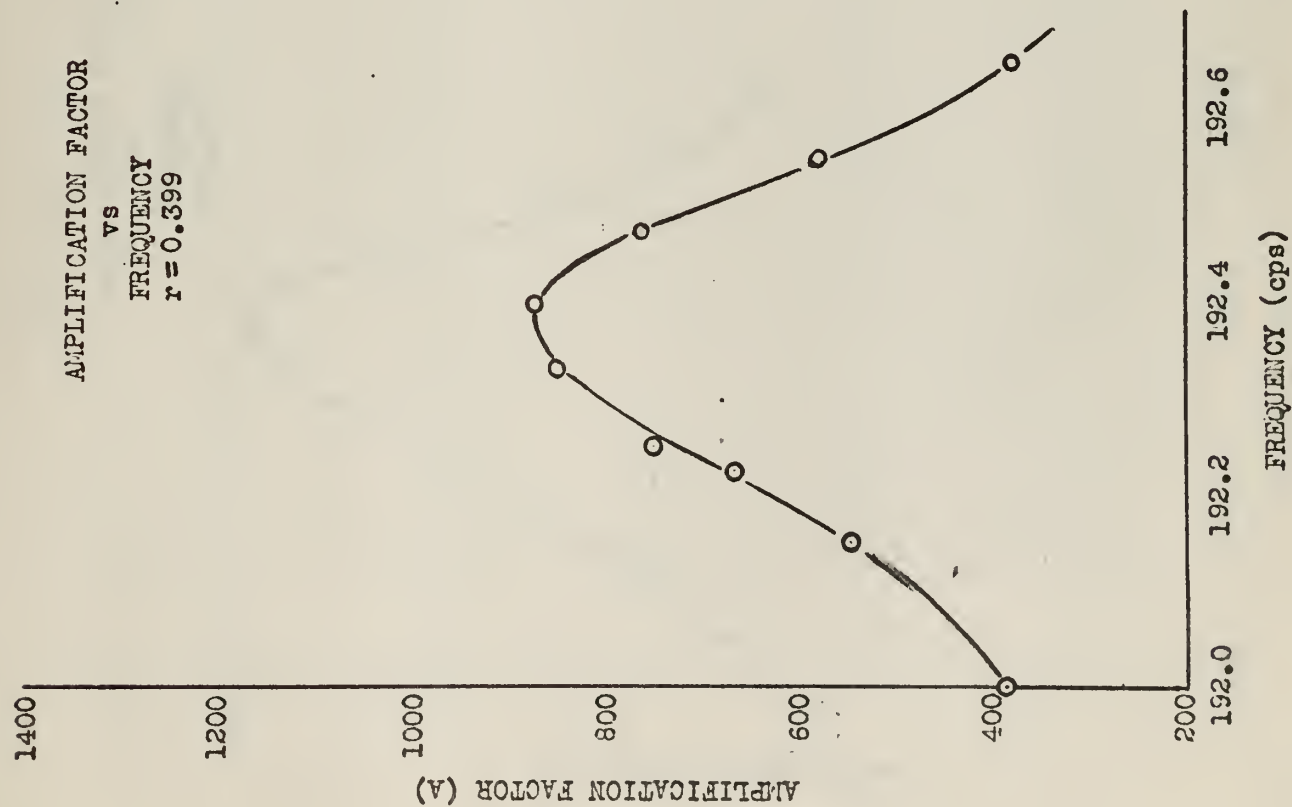


FIG. 10

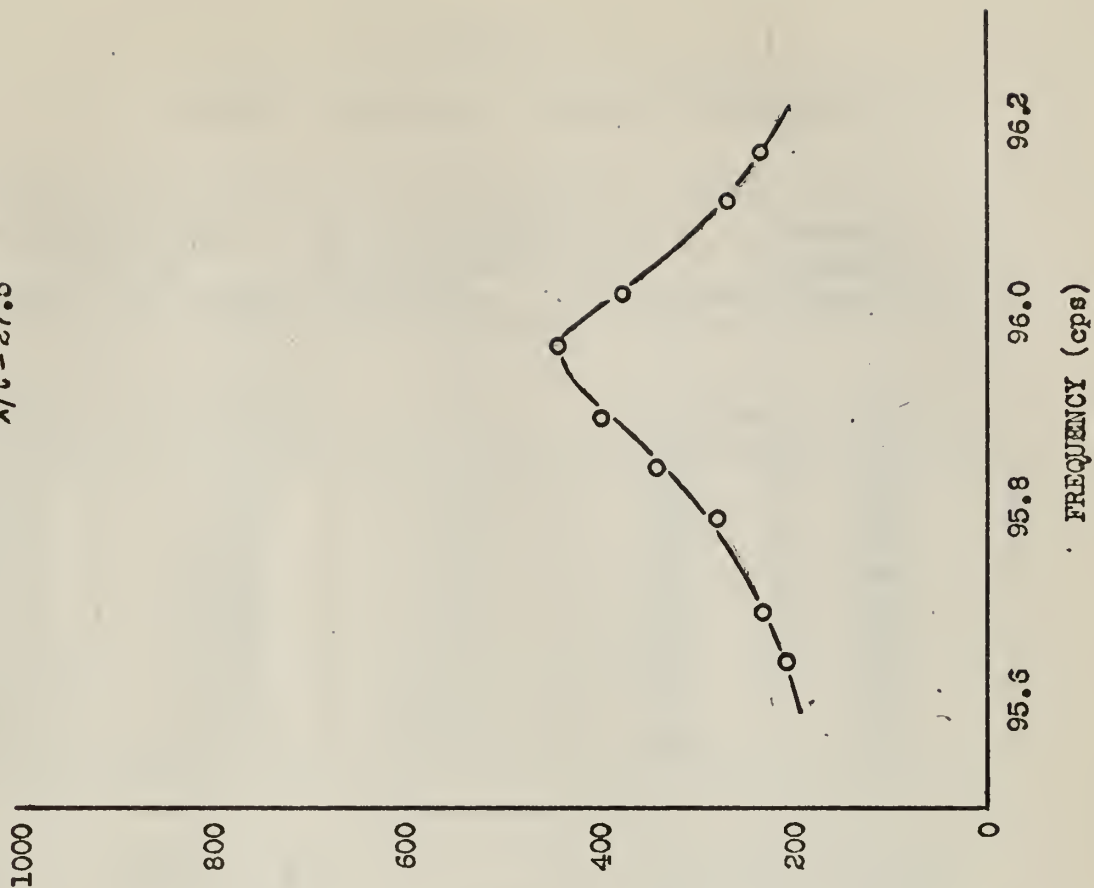
AMPLIFICATION FACTOR

vs

FREQUENCY

$r = 0.275$

$\lambda/t = 27.5$



AMPLIFICATION FACTOR

vs

FREQUENCY

$r = 0.803$

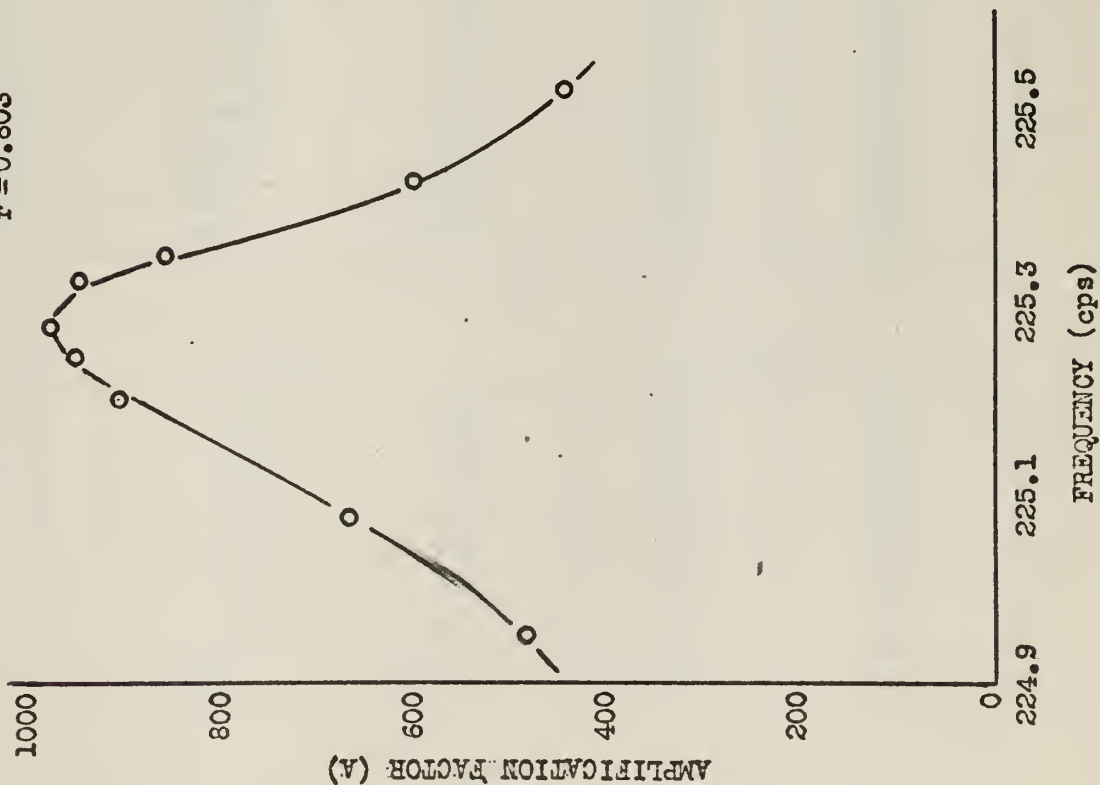


FIG. 11

TABLE VI
STEADY STATE FORCED VIBRATION EXPERIMENTAL DATA

Root Amplitude a_0		Tip Amplitude y_0		Resonant Amplification Factor A_r
millivolts	10^{-6} inches	microscope divisions	10^{-3} inches	

Solid Beam $f_n = 166.0$ cps

V ambient = 0.045 mv

0.30	2.42	4.4	2.40	990
0.50	4.03	6.0	3.63	900
0.60	4.84	7.0	4.40	910
0.70	5.66	7.8	5.00	880
0.80	6.45	8.2	5.32	820
0.90	7.28	9.0	5.94	815
1.00	8.11	9.8	6.57	810
1.20	9.68	10.2	7.63	790
1.50	12.13	12.8	8.85	730

$r = 0.260$ $f_n = 181.7$ cps

V ambient = 0.045 mv

0.60	4.05	5.0	3.32	820
0.70	4.72	5.5	3.78	800
0.80	5.39	6.2	4.25	790
0.90	6.06	6.7	4.62	760
1.00	6.73	7.2	5.00	740
1.25	8.43	8.7	5.63	670
1.50	10.12	9.2	6.57	650
2.00	15.5	10.5	7.55	560
3.00	20.3	12.5	9.10	450
3.50	25.6	15.3	9.72	410

$r = 0.399$ $f_n = 192.4$ cps

V ambient = 0.04 mv

0.50	3.05	3.8	2.54	845
0.60	3.61	4.5	3.08	855
0.71	4.25	5.3	3.71	870
0.90	5.41	6.6	4.70	870
1.00	6.02	7.0	5.01	835
1.25	7.52	8.8	6.40	850
1.50	9.01	10.4	7.63	845
2.00	12.0	12.5	9.25	770
2.50	15.1	14.4	10.70	710

TABLE VI (cont.)

Root Amplitude		Tip Amplitude		Resonant Amplification Factor A_r
millivolts	10^{-6} inches	microscope divisions	10^{-3} inches	

 $r = 0.516$ $f_n = 195.6$ cps $V_{\text{ambient}} = 0.045$ mv

0.60	3.50	7.5	5.23	1500
0.70	4.07	8.0	5.62	1330
0.80	4.66	9.0	6.40	1375
0.91	5.30	9.7	6.94	1310
1.00	5.82	10.3	7.40	1270
1.25	7.28	11.8	8.56	1175
1.50	8.74	13.6	9.95	1140
2.00	11.7	15.8	11.6	1000
2.52	14.7	17.8	13.2	900
3.00	17.5	19.3	14.7	845

 $r = 0.803$ $f_n = 225.3$ cps $V_{\text{ambient}} = 0.045$ mv

0.50	2.20	3.2	2.24	985
0.75	3.27	4.4	3.18	965
1.00	4.53	5.9	4.33	995
1.20	5.23	6.9	5.10	975
1.40	6.13	8.2	6.10	995
1.60	7.00	9.2	6.87	980
1.80	7.91	10.0	7.48	945
2.00	8.78	11.0	8.26	940
2.50	11.0	13.2	9.95	910
3.00	13.2	15.3	11.6	880
4.00	17.6	20.0	15.1	865

 $r = 0.257$ $\lambda/t = 27.5$ $f_n = 95.9$ cps $V_{\text{ambient}} = 0.045$ mv

0.37	8.92	6.1	3.94	440
0.50	12.1	7.9	5.32	440
0.78	18.9	11.4	8.02	425
0.98	23.7	14.8	10.6	450
1.23	31.0	19.0	13.9	450

TABLE VII
FREE VIBRATION DECAY EXPERIMENTAL DATA

Run	f	X ₀	X _n	X _{2n}	X _{3n}	X _{4n}	n	y ₀	δ
	cps	Inches					cycles	average	

Solid Beam

1	166.4	3.99	3.48	3.046	2.63	-	40	0.0067	0.0069
2	166.3	4.04	3.54	3.12	2.77	2.40	40	0.0069	0.0065
3	166.2	4.14	3.52	2.96	2.48	2.30	40	0.0069	0.0075
1		2.63	2.35	2.07	1.82	-	40	0.0046	0.0062
2		2.11	1.86	1.66	1.44	1.26	40	0.0037	0.0063
3		1.76	1.56	1.34	1.15	1.01	40	0.0032	0.0069

$$r = 0.260$$

1	180.3	2.48	2.00	1.72	1.43	-	40	0.0045	0.0092
2	179.4	2.40	1.97	1.66	1.41	-	40	0.0060	0.0089
3	179.3	2.72	2.29	1.85	1.51	-	40	0.0047	0.0098
1		1.16	1.00	0.85	0.70	-	40	0.0041	0.0082
2		1.20	1.01	0.86	0.75	-	40	0.0041	0.0080
3		1.51	1.24	1.04	-	-	40	0.0039	0.0072

$$r = 0.399$$

1	192.1	3.80	3.42	3.08	2.76	2.48	20	0.0079	0.0053
2	192.1	3.30	2.78	2.42	2.06	1.72	30	0.0065	0.0054
3	191.8	3.70	3.15	2.68	-	-	30	0.0080	0.0054
1		2.48	2.24	2.02	1.81	-	20	0.0054	0.0052
2		1.72	1.50	1.28	1.10	-	30	0.0035	0.0052
3		1.96	1.69	1.42	1.22	-	30	0.0040	0.0053

$$r = 0.516$$

1	194.3	2.83	2.20	1.64	1.25	-	30	0.0080	0.0091
2	194.2	2.32	1.85	1.33	1.04	-	30	0.0066	0.0089
3	194.4	2.52	1.95	1.56	-	-	30	0.0080	0.0080
1		1.25	0.98	0.78	0.62	0.49	30	0.0034	0.0079
2		0.76	0.62	0.48	-	-	30	0.0029	0.0082
3		1.56	1.27	1.00	-	-	30	0.0050	0.0074

TABLE VII (cont.)

Run	f	X_0	X_n	X_{2n}	X_{3n}	X_{4n}	n	γ_0	δ
	cps	Inches					cycles	average	

$r = 0.803$

1	224.3	2.87	2.45	1.64	1.53	1.28	20	0.0125	0.0104
2	224.2	2.95	2.09	1.39	-	-	20	0.0127	0.0154
3	224.2	2.36	1.96	1.59	-	-	20	0.0115	0.0098
1		1.00	0.90	0.73	0.47	0.35	20	0.0048	0.0104
2		.99	0.76	0.57	0.42	-	20	0.0041	0.0127
3		1.38	1.24	1.12	-	-	20	0.0073	0.0052

$r = 0.257$ $\lambda/t = 27.5$.

1	96.1	2.62	2.08	1.77	1.45	1.13	10	0.0202	0.0210
2	96.2	2.55	2.34	1.66	1.32	-	10	0.0202	0.0219
3	96.3	3.54	3.04	2.53	2.24	1.93	10	0.0218	0.0151
4	96.2	2.90	2.48	2.06	-	-	10	0.0211	0.0170
1		1.13	0.93	0.76	0.62	-	10	0.0072	0.0200
2		1.06	0.84	0.72	0.58	0.47	10	0.0075	0.0203
3		1.65	1.45	1.25	1.06	0.84	10	0.0098	0.0141
4		2.06	1.76	1.54	1.26	1.08	10	0.0091	0.0161

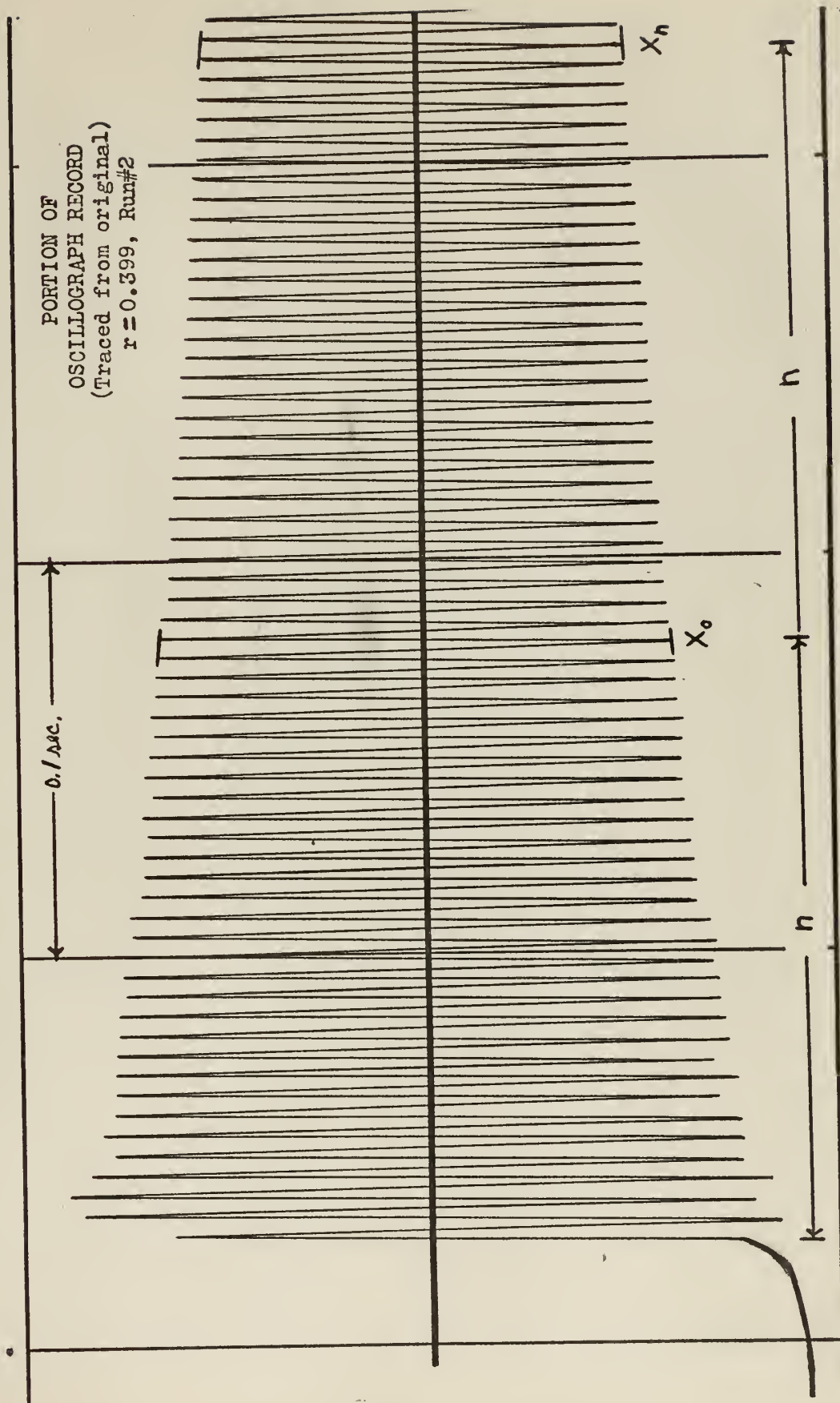
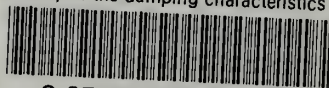


FIG. 12

thesV165

A study of the damping characteristics o



3 2768 002 05369 6

DUDLEY KNOX LIBRARY